

# Design, synthesis, and screening of *ortho*-amino thiophene carboxamide derivatives on hepatocellular carcinoma as VEGFR-2 inhibitors

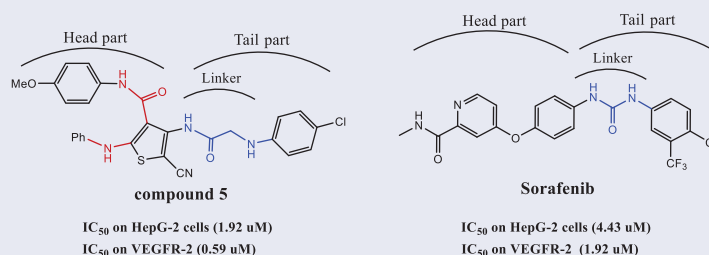
Mohammed K. Abdelhameid<sup>a</sup>, Madlen B. Labib<sup>b</sup>, Ahmed T. Negmeldin<sup>a,c</sup> , Muhammad Al-Shorbagy<sup>d,e</sup> and Manal R. Mohammed<sup>f</sup>

<sup>a</sup>Pharmaceutical Organic Chemistry Department, Faculty of Pharmacy, Cairo University, Cairo, Egypt; <sup>b</sup>Department of Pharmaceutical Organic Chemistry, Faculty of Pharmacy, Beni-Suef University, Beni-Suef, Egypt; <sup>c</sup>Department of Pharmaceutical Sciences College of Pharmacy, Gulf Medical University, Gulf Medical University, Ajman, UAE; <sup>d</sup>Pharmacology and Toxicology Department, Faculty of Pharmacy, Cairo University, Cairo, Egypt; <sup>e</sup>Pharmacology and Toxicology Department, School of Pharmacy, NewGiza University, Egypt; <sup>f</sup>Department of Radiation Biology, National Center for Radiation Research and Technology, Cairo, Egypt

## ABSTRACT

In this work, design, synthesis, and screening of thiophene carboxamides **4–13** and **16–23** as dual vascular endothelial growth factor receptors (VEGFRs) and mitotic inhibitors was reported. All compounds were screened against two gastrointestinal solid cancer cells, HepG-2 and HCT-116 cell lines. The most active cytotoxic derivatives **5** and **21** displayed 2.3- and 1.7-fold higher cytotoxicity than Sorafenib against HepG-2 cells. Cell cycle and apoptosis analyses for compounds **5** and **21** showed cells accumulation in the sub-G1 phase, and cell cycle arrest at G2/M phase. The apoptotic inducing activities of compounds **5** and **21** were correlated to the elevation of p53, increase in Bax/Bcl-2 ratio, and increase in caspase-3/7. Compounds **5** and **21** showed potent inhibition against VEGFR-2 ( $IC_{50}$  = 0.59 and 1.29  $\mu$ M) and  $\beta$ -tubulin polymerization (73% and 86% inhibition at their  $IC_{50}$  values). Molecular docking was performed with VEGFR-2 and tubulin binding sites to explain the displayed inhibitory activities.

## GRAPHICAL ABSTRACT



## ARTICLE HISTORY

Received 20 March 2018  
Revised 21 June 2018  
Accepted 16 July 2018

## KEYWORDS

Gastrointestinal carcinoma;  
HepG-2; HCT-116;  
thiophene carboxamide;  
 $\beta$ -tubulin; angiogenesis

## 1. Introduction

Adenocarcinoma as hepatocellular carcinoma (HCC) and colorectal cancer are highly vascularized solid tumours characterized by angiogenesis signaling pathway abnormalities<sup>1,2</sup>. Vascular endothelial growth factor receptors (VEGFRs) are receptor tyrosine kinases (RTKs) that are implicated in angiogenesis. Reduction of angiogenesis via inhibition of the pro-angiogenic enzymes as VEGFR-2, have become the focus of a new wave of targeted chemotherapy for adenocarcinoma<sup>3</sup>.

Despite of promising clinical outcomes of the angiokinase inhibitors as Sorafenib (Nexavar)<sup>TM</sup> and Regorafenib (Stivarga)<sup>TM</sup> (Figure 1) in HCC and colon cancer chemotherapy<sup>4</sup>, both tumours are still considered among the leading causes of mortality worldwide<sup>1,2,4–6</sup>. Generally, RTK inhibitors are either ATP competitive or noncompetitive inhibitors according to the binding mode to

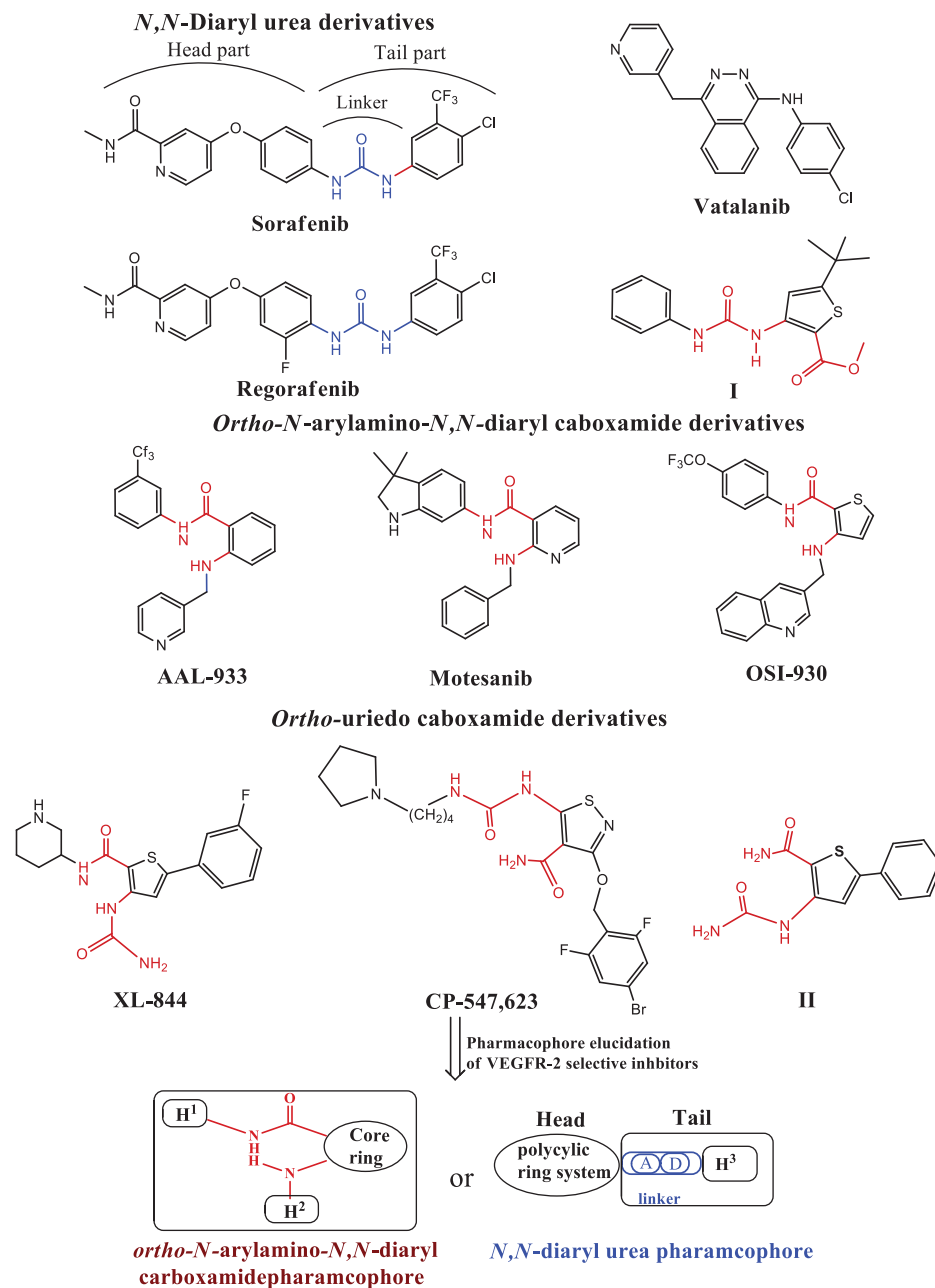
kinase domain<sup>7,8</sup>. ATP competitive inhibitors bind to ATP enzyme binding pocket, while noncompetitive inhibitors bind to ATP binding pocket, in addition to the allosteric binding site adjacent to the ATP pocket<sup>9</sup>. Competitive inhibitors are structurally composed of orthogonal biaryl ring system with pharmacophoric features<sup>10</sup> including hydrogen bond (H-bond) acceptor–donor pair forming groups (A and D) that interact with the kinase “hinge” region, in addition to two hydrophobic groups (H1 and H2) around the region occupied by the ATP adenine ring. Vatalanib (Figure 1) is an example of competitive RTK inhibitors regarded as first generation VEGFR inhibitors<sup>11</sup>. that lack VEGFR selectivity specifically VEGFR-2 such accounts to pronounced side effects<sup>12</sup>. Noncompetitive inhibitors as Sorafenib represent the second generation of RTK inhibitors, are composed of two parts: (i) head part with similar structural features of ATP binding competitors and is

**CONTACT** Ahmed T. Negmeldin [ahmed.n@pharma.cu.edu.eg](mailto:ahmed.n@pharma.cu.edu.eg) Pharmaceutical Organic Chemistry Department, Faculty of Pharmacy, Cairo University, 33 Kasr El-Aini, Cairo 11562, Egypt

Supplemental data for this article can be accessed [here](#).

© 2018 The Author(s). Published by Informa UK Limited, trading as Taylor & Francis Group.

This is an Open Access article distributed under the terms of the Creative Commons Attribution-NonCommercial License (<http://creativecommons.org/licenses/by-nc/4.0/>), which permits unrestricted non-commercial use, distribution, and reproduction in any medium, provided the original work is properly cited.



Core ring is aryl group, H<sup>1</sup>, H<sup>2</sup> and H<sup>3</sup> are hydrophobic aryl groups, head is orthogonal or fused polycyclic rings,

Tail is hydrophobic aryl group H<sup>3</sup> with linker part (amide or urea) as hydrogen bond interacting groups

**Figure 1.** Chemical structures of the lead receptor tyrosine kinases (RTKs) inhibitors. *ortho*-amino-aryl carboxamide and *ortho*-uriedoaryl caboxamide pharmacophores showed in red color, urea pharmacophore as linker showed in blue color.

responsible for potency and binding to the ATP binding site<sup>13</sup> and (ii) tail part which binds to the allosteric site via H-bond forming linkers (amide or urea moieties) having a H-bond acceptor donor pair, and links the head part to another aryl group forming hydrophobic interactions (H3)<sup>9,13</sup>. Structural biology investigation performed on the complexes between vatalanib and the catalytic domain of the enzyme led to the discovery of AAL-993 (Figure 1), that belongs structurally to the *ortho-N*-aryl-amino-*N,N*-diaryl carboxamides<sup>14</sup>. Several novel VEGFR kinase inhibitors (Figure 1) were identified as anti-cancer agents with close structural similarities to the aforementioned drug possessing different heterocyclic cores, such as Motesanib (*ortho-N*-aryl-2-amino-*N'*-arylpyridine-3-carboxamide)<sup>15</sup>, OSI-930 (*ortho-N*-aryl-3-amino-*N'*-arylthiophene-2-carboxamide)<sup>16,17</sup>. XL-844 (*ortho*-3-

uriedothiophene-2-carboxamide) which was reported as a synthetic small-molecule with dual checkpoint and angiokine inhibition activities<sup>18</sup>, and CP-547,632 (*ortho*-5-ureidoisothiazole-4-carboxamide)<sup>18</sup>. Discovery of the previous drugs proceeded a novel wave of selective VEGFR-2 kinase inhibitors as anti-angiogenic agents with low affinity against other RTKs, which are structurally based upon either *ortho-N*-arylamino-*N,N'*-diarylamide or *ortho*-ureido-*N,N'*-diarylamide pharmacophoric moieties. Earlier, the prototype RTK inhibitor (*N*-aryl-3-thienyl urea **I**)<sup>19</sup>. (Figure 1) was reported as B-Raf kinase inhibitor and provided a route to the discovery of sorafenib. Unfortunately, although second generation VEGFR-2 inhibitors have the advantage of being selective enzyme inhibitors towards VEGF pathway other than malignant angiogenesis pathways, they face a major therapy problems as tumour cells can tolerate the

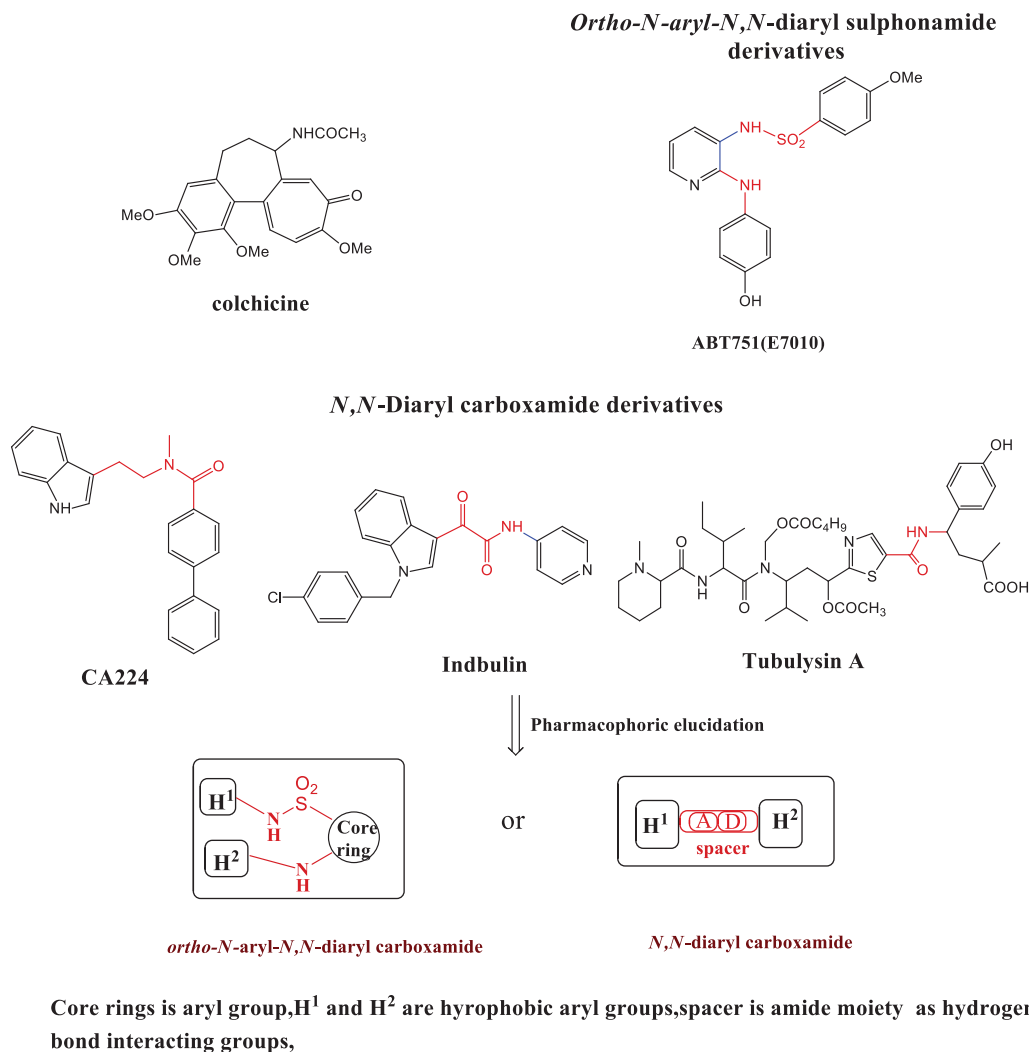


**Figure 2.** Chemical structures of some anti-mitotic drugs via tubulin polymerization inhibition. *ortho*-amino-aryl sulphonamide and diaryl caboxamide pharmacophores showed in red color.

drug induced hypoxia and hence acquire resistance to apoptosis induction<sup>20,21</sup>. Consequently, these drugs are used in high doses in advanced treatment<sup>22</sup>, causing severe drawbacks on patients' lives quality. Thus, second generation VEGFR inhibitors are usually used in combination with other drugs targeting more than growth signaling pathways in order to promote apoptosis<sup>22</sup>. A drawback of combination therapy is the increased risk of side effects of both drugs<sup>22</sup>. As an alternative therapeutic approach, novel small molecule compounds with dual targets could successfully lead to the desired cytotoxic effect with minimal side effects leading to a better life quality for cancer patients<sup>23</sup>. Interestingly, combination chemotherapy of anti-angiogenesis agents with antimitotic drugs increased cytotoxicity to tumour cells without adding toxicity to normal cells, which led to reduced side effects associated with the chemotherapy<sup>24</sup>. To discover pharmacophoric moieties that could be added to the core structure of anti-angiogenic agents, we studied colchicine binding site inhibitors, as the most commonly explored target for antimitotic drugs which are considered as one of the most successful targets for cancer chemotherapy<sup>25,26</sup>. Inhibiting cell division *via* suppression of microtubules growth, prevention of tubulin polymerization, blocking G2/M phase of the cell cycle and promoting apoptosis<sup>27</sup>. Various drugs (Figure 2) were reported as potent antimitotic agents with common structural similarities such as ABT-751 (*ortho*-N-arylamino-

*N'*-aryl-benzenesulphonamide)<sup>28</sup>, a drug in phase II clinical trials that binds to the colchicine binding site for treatment of lung and prostate cancer, CA224 (*N,N*-alkylhetoroaryl carboxamide)<sup>29</sup>, Indibulin (*N,N'*-diaryl glyoxyl-amide)<sup>29</sup>, which was reported for treatment of solid tumours, and the natural product Tubulysin A<sup>30</sup>. Colchicine binding site inhibitors (CSIs) are categorized into typical CSIs, as colchicines (Figure 2), and atypical CSIs as EBT-751. The essential pharmacophoric features of typical CSIs are: biaryl ring system, methoxyphenyl fragment, and a restricted conformation moiety while atypical CSIs lack at least one of these features<sup>31</sup>. There are seven pharmacophoric points in colchicine binding site: three H-bond acceptors, one H-bond donor, two hydrophobic centers (H1, H2) and one planar group. The two hydrophobic and planar groups are responsible for the molecular skeleton and structural rigidity, while H-bond acceptor donor pair groups increase receptor binding interactions<sup>32</sup>. Surprisingly, although colchicine is a fused polycyclic compound, colchicine binding site is a folded architecture where, four points are in one plane, and three points are in a second plane. For this reason, complete planar anthracene and phenanthrene frameworks -analogs of colchicine- are inactive<sup>33</sup>. Hence, the design of the non-fused polycyclic flexible molecule is advantageous over fused planar polycyclic molecules. Since none of the known CSI structural models including colchicines occupy the seven pharmacophoric

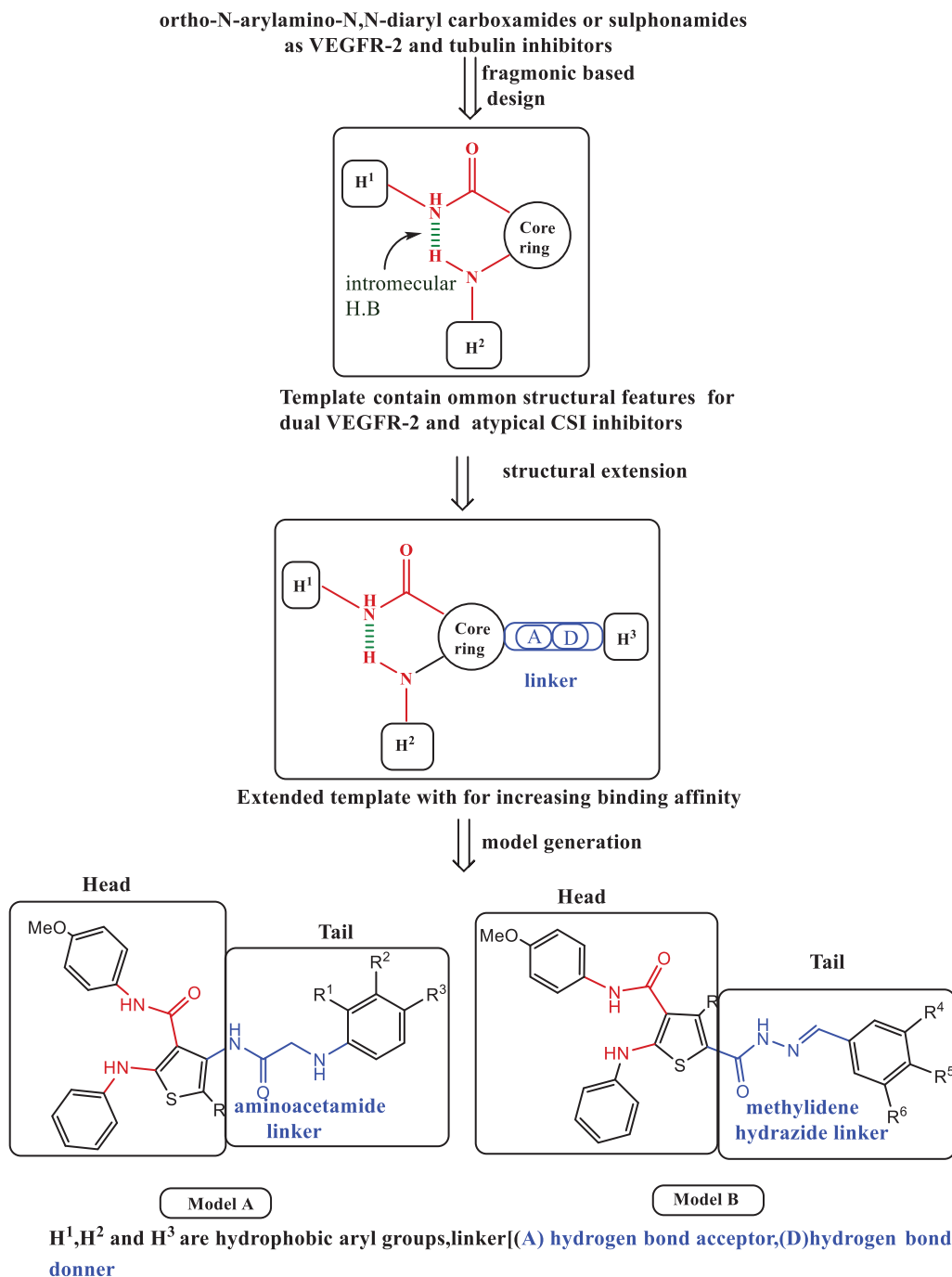


**Figure 3.** Diagrammatic sketch for molecular design strategy for elucidation of dual pharmacophoric template and structural extension of the template with the generation of the two models; Model A, substituted phenyl acetamides 4–13 and Model B substituted arylidene hydrazides 16–23. *ortho*-amino-aryl caboxamide pharmacophore showed in red color, isosteric groups (2-amino-acetamide and methyldene hydrazide) to urea pharmacophore as linker showed in blue color.

points<sup>31</sup>, the design of novel hit molecules with increased binding affinity towards colchicine binding site is an interesting target in the field of medicinal chemistry research. Based on the history of drug discovery, we found that some drugs having common functional fragments often exhibit extended biological activities<sup>34</sup>. Inspecting the structure of the mentioned antimitotic agents showed that they have similar constitutional characters to the mentioned VEGFR inhibitors where the *N,N*-diaryl carboxamide and *ortho*-amino-*N,N'*-diaryl sulfonamide are isosters to each other (Figure 3). The biological activities of these drugs may be explained based upon their structure as it can form intramolecular H-bond between the *ortho*-disubstituted *N*-aryl amino-*N*-aryl carboxamide groups on the core ring. This pseudo

fused ring system could simulate the adenine ring of ATP and the polycyclic ring skeleton of colchicine in interaction with binding sites. The observed structural similarities between VEGFR and tubulin polymerization inhibitors have stimulated our efforts to use the fragment-based lead generation approach<sup>35</sup>. to design and synthesize dual VEGFR and  $\beta$ -tubulin polymerization inhibitors towards the road for discovery of potent third generation VEGFR inhibitors. Fragment-based lead generation approach is one of the leading methods in drug design and applied by identification of biological active fragments in drugs used in the market in order to generate novel lead structures<sup>35</sup>. Moreover, multi-targeted enzyme inhibitors are one of the hot topics in cancer drug discovery aiming to increase

cytotoxicity by synergistic effect towards tumour cells and also to decrease cancer cells resistance to apoptosis induction<sup>36,37</sup>. Combined with our previous studies on HCC and dual cytotoxic agents<sup>38,39</sup>, we attempted to combine anti-angiogenic and tubulin inhibition activities into several derivatives by using a common pharmacophoric moiety (*ortho*-*N*-arylamino-*N,N*-diaryl carboxamide) as a template to act as a dual angiokinase and tubulin polymerization inhibitor. To increase the binding of the novel molecules to both biological targets, the structure of the template is enriched with additional kinase and colchicine site interacting moieties. Structural extension of the common template resulted in two models (A and B), both of them have head and tail parts (Figure 3). The head part (*ortho*-amino-*N,N*-diaryl carboxamide) is a common pharmacophore present to fulfill the basic requirement of VEGFR and colchicine binding site inhibitors. The tail part in both models is added to increase binding affinity to kinase and tubulin polymerization binding sites, and is formed from linker groups attached to aryl rings. The structure of tail parts has pharmacophoric similarities with ligands that bind to VEGFR and colchicine binding sites deduced from the known drugs Sorafenib and seven pharmacophoric features of CSI inhibitors. For instance, the 2-amino-acetamide group in model A is similar to the ureido group of sorafenib, in addition to the presence of methoxylated aryl ring and rigid configuration in model B to reach seven pharmacophoric points. Also, linkers used in both models differ in rigidity, where 2-amino-acetamide moiety is a flexible linker in model A, while methyldiene hydrazide fragment is a restricted linker in model B. On the other hand, they have some similar structural features, such as the distance between head part and aryl groups in tail part and the capability of H-bond formation (acceptor–donor pair) that increase the interaction with binding sites. In Model A (*N,N'*-diaryl-2-amino-acetamide thiophenes **4–13**), the isosteric 2-amino-acetamide group increases the probability to anchor colchicine and kinase binding sites by H-bond formation. In Model B (*N*-arylidene thiophene hydrazides **16–23**), methyldiene hydrazide constitute a rigid link to possess the model a restricted conformation property as that present in colchicine with the similar length and H-bond formation characters present in model A. The rigid configuration will help the model to possess the correct orientation to fit in both binding sites. Moreover, the aryl groups of the tail part were endowed with different electron withdrawing (halogens) or donating (hydroxyl or methoxy) groups to investigate the effect of substituents on the binding (Figure 3). It is worthy to note that unsubstituted thiophene derivatives are metabolically unstable and toxic due to formation of irreversible bond interaction with cytochrome p450, therefore the head part in both models contain oxidation protecting groups (nitrile or carbamyl) as electron withdrawing substituents to increase the stability of thiophene ring against metabolic oxidation<sup>40,41</sup>.

## 2. Experimental

### 2.1. Chemical synthesis

#### 2.1.1. General

Melting points (°C, uncorrected) were determined in open capillaries on a Graffin melting point apparatus. Pre-coated silica gel plates (silica gel 0.25 mm, 60 G F 254; Merck, Germany) were used for thin layer chromatography, dichloromethane/methanol (9.5:0.5 ml) mixture was used as a developing solvent system. IR spectra were recorded as films on KBr discs using IR-470 Shimadzu spectrometer (Shimadzu, Tokyo, Japan). The NMR spectra were recorded by Varian Gemini-300BB 300 MHz FT-NMR

spectrometers (Varian Inc., Palo Alto, CA). <sup>1</sup>H and <sup>13</sup>C spectra were run at 300 and 75 MHz, respectively, in deuterated dimethylsulfoxide (DMSO-*d*<sub>6</sub>). Chemical shifts ( $\delta_{\text{H}}$ ) are reported relative to TMS as internal standard. All coupling constant (*J*) values are given in hertz. Chemical shifts ( $\delta_{\text{C}}$ ) are reported relative to DMSO-*d*<sub>6</sub> as internal standards. Elemental analysis was performed on Carlo Erba 1108 Elemental Analyzer (Heraeus, Hanau, Germany). Electron impact Mass Spectra (EIMS) were recorded on Hewlett Packard 5988 spectrometer, Micro analytical center, Cairo University, Cairo. All compounds were within  $\pm 0.4\%$  of the theoretical values. All solvents and reagents were commercially available and used without further purification. Sieno-Mass-II microwave (2.45GHz, 1000W) synthesis workstation was used. 2-Cyano-*N*-(4-methoxyphenyl) acetamide**1** was prepared as reported<sup>42</sup>.

#### 2.1.2. General procedure for synthesis of 4-amino-*N*-(4-methoxyphenyl)-5-substituted-2-phenylaminothiophene-3-carboxamides (**2a** and **b**)

To a stirred solution of anilide**1** (1.9 g, 0.01 mol) in absolute ethanol (20 ml), an ethanolic solution of sodium ethoxide (0.23 g sodium, 0.01 mol, 4 ml absolute ethanol) was added drop-wise and reaction mixture was stirred at room temperature. After 2 h, phenyl isothiocyanate (1.35 g, 0.01 mol) was added and the mixture was heated for 30 min at 70 °C then cooled to 25 °C. The  $\alpha$ -chloromethylene derivative (0.01 mol) was then added, and the temperature raised to 60 °C for another 30 min. Sodium ethoxide (0.12 g sodium, 0.005 mol, 5 ml absolute ethanol) was then added and heating was continued under reflux temperature for additional 3 h. After cooling to room temperature, the reaction mixture was poured into ice cold water, the separated product was filtered, dried and recrystallized from ethanol to afford compounds **2a** and **2b**.

**2.1.2.1. 4-Amino-5-cyano-*N*-(4-methoxyphenyl)-2-phenylaminothiophene-3-carboxamide (2a).** Yield 62% (2.25 g); mp 291–293 °C; IR (KBr,  $\nu$  cm<sup>-1</sup>): 3356–3224 (2NH, NH<sub>2</sub>), 2186 (C≡N), 1644 (C=O). <sup>1</sup>H NMR (DMSO-*d*<sub>6</sub>): 3.67 (s, 3H, OCH<sub>3</sub>), 7.04–7.13 (m, 3H, Ar-H), 7.29–7.35 (m, 4H, Ar-H), 7.62 (d, *J* = 8.4 Hz, 2H, Ar-H), 9.74 (s, 1H, NH, D<sub>2</sub>O exchangeable), 9.89 (s, 1H, D<sub>2</sub>O exchangeable), 10.18 (s, 2H, NH<sub>2</sub>, D<sub>2</sub>O exchangeable). MS (*m/z*, %): 364 (M<sup>+</sup>, 6.60), 123 (100). Anal. Calcd. for C<sub>19</sub>H<sub>16</sub>N<sub>4</sub>O<sub>2</sub>S (364.42): C, 62.62; H, 4.43; N, 15.37. Found: C, 62.75; H, 4.37; N, 15.43.

**2.1.2.2. Ethyl-3-amino-4-(4-methoxyphenylcarbamoyl)-5-phenylaminothiophene-2-carboxylate (2b).** Yield 73% (3 g); mp >300 °C; IR (KBr,  $\nu$  cm<sup>-1</sup>): 3340–3262 (2NH, NH<sub>2</sub>), 1667–1625 (2C=O). <sup>1</sup>H NMR (DMSO-*d*<sub>6</sub>): 1.21 (t, *J* = 6.9 Hz, 3H, OCH<sub>2</sub>CH<sub>3</sub>), 3.74 (s, 3H, OCH<sub>3</sub>), 4.14 (q, *J* = 6.9 Hz, 2H, OCH<sub>2</sub>CH<sub>3</sub>), 6.68 (s, 2H, NH<sub>2</sub>, D<sub>2</sub>O exchangeable), 7.09–7.12 (m, 3H, Ar-H), 7.30–7.39 (m, 4H, Ar-H), 7.50 (d, *J* = 8.4 Hz, 2H, Ar-H), 9.63 (s, 1H, NH, D<sub>2</sub>O exchangeable), 9.69 (s, 1H, NH, D<sub>2</sub>O exchangeable). MS (*m/z*, %): 412 (M<sup>+</sup> + 1<sup>+</sup>, 9.65), 411 (M<sup>+</sup>, 18.70), 123 (100). Anal. Calcd. for C<sub>21</sub>H<sub>21</sub>N<sub>3</sub>O<sub>4</sub>S (411.47): C, 61.30; H, 5.14; N, 10.21. Found: C, 61.17; H, 5.26; N, 10.19.

#### 2.1.3. Procedure for synthesis of 4-(2-chloro-acetamido)-5-cyano-*N*-(4-methoxyphenyl)-2-phenylaminothiophene-3-carboxamide (**3**)

To a stirred solution of 4-aminothiophene-3-carboxamide derivative (**2a**, 0.55 g, 0.0015 mol) in *n*-butanol (5 ml), chloroacetyl chloride (0.17 g, 0.0015 mol) was added drop-wise with cooling at room temperature and the mixture was irradiated in the microwave oven at 150 °C for 5 min. After cooling to room temperature, the mixture was diluted with petroleum ether (5 ml). The solid formed



was collected and treated with sodium carbonate solution (10%, 2 ml) then filtered, washed with water, dried and recrystallized from ethanol to afford white crystals of 4-(2-chloroacetamido)-thiophene-3-carboxamide derivative **3**. Yield 59% (0.39 g); mp 242–244 °C; IR (KBr,  $\nu$  cm<sup>-1</sup>): 3417–3234 (3NH), 2200 (C≡N), 1678–1628 (2C=O). <sup>1</sup>H NMR (DMSO-*d*<sub>6</sub>): 3.63 (s, 3H, OCH<sub>3</sub>), 4.83 (s, 2H, CH<sub>2</sub>Cl), 7.05–7.16 (m, 2H, Ar-H), 7.24–7.50 (m, 3H, Ar-H), 7.59 (d, *J* = 8.1 Hz, 2H, Ar-H), 7.73 (d, *J* = 7.8 Hz, 2H, Ar-H), 10.56 (s, 1H, NH, D<sub>2</sub>O exchangeable), 10.81 (s, 1H, NH, D<sub>2</sub>O exchangeable), 11.21 (s, 1H, NH, D<sub>2</sub>O exchangeable). MS (*m/z*, %): 442 (M + 2<sup>+</sup>, 8.27), 441 (M + 1<sup>+</sup>, 10.84), 440 (M<sup>+</sup>, 27.58), 267 (100). Anal. Calcd. for C<sub>21</sub>H<sub>17</sub>ClN<sub>4</sub>O<sub>3</sub>S (440.90): C, 57.21; H, 3.89; N, 12.71. Found: C, 57.39; H, 3.92; N, 12.68.

#### 2.1.4. General procedure for synthesis of 5-cyano-N-(4-methoxyphenyl)-2-phenylamino-4-(2-aryl-amino-acetamido)thiophene-3-carboxamides (4–13)

To a stirred solution of 4-(2-chloroacetamido)thiophene-3-carboxamide **3** (0.44 g, 0.001 mol) in ethylene glycol (5 ml), the appropriate aromatic amine (0.002 mol) was added. The reaction mixture was irradiated in microwave oven at 120 °C for 15 min. After cooling to room temperature, the reaction mixture was diluted with petroleum ether (5 ml) and the precipitated solid was filtered, dried, and recrystallized from proper solvent to afford 4-(2-aryl-amino-acetamido)thiophene-3-carboxamides **4–13**.

**2.1.4.1. 5-Cyano-N-(4-methoxyphenyl)-2-phenylamino-4-(2-phenyl-amino-acetamido)thiophene-3-carboxamide (4).** Yield 76% (0.37 g); mp 233–236 °C (EtOH); IR (KBr,  $\nu$  cm<sup>-1</sup>): 3425–3243 (4NH), 2210 (C≡N), 1665–1630 (2C=O). <sup>1</sup>H NMR (DMSO-*d*<sub>6</sub>):  $\delta$  3.73 (s, 3H, OCH<sub>3</sub>), 4.82 (s, 2H, CH<sub>2</sub>), 7.07–7.13 (m, 5H, Ar-H), 7.29–7.32 (m, 3H, Ar-H), 7.35–7.41 (m, 4H, Ar-H), 7.58 (d, *J* = 8.4 Hz, 2H, Ar-H), 9.58 (s, 1H, NH, D<sub>2</sub>O exchangeable), 10.56 (s, 1H, NH, D<sub>2</sub>O exchangeable), 10.81 (s, 1H, NH, D<sub>2</sub>O exchangeable), 11.26 (s, 1H, NH, D<sub>2</sub>O exchangeable). <sup>13</sup>C NMR (DMSO-*d*<sub>6</sub>):  $\delta$  54.9 (CH<sub>2</sub>), 55.6 (OCH<sub>3</sub>), 67.9, 97.8, 112.9 (C≡N), 119.0, 123.0, 123.5, 128.8, 129.2, 131.3, 136.4, 136.9, 138.5, 143.1, 147.6, 148.1, 156.1, 163.7, 165.8, 166.9. Anal. Calcd. for C<sub>27</sub>H<sub>23</sub>N<sub>5</sub>O<sub>3</sub>S (497.15): C, 65.17; H, 4.66; N, 14.08; Found: C, 65.00; H, 4.40; N, 13.88.

**2.1.4.2. 4-[2-(4-Chlorophenyl)aminoacetamido]-5-cyano-N-(4-methoxyphenyl)-2-phenylaminothiophene-3-carboxamide (5).** Yield 72% (0.38 g); mp 210–212 °C (EtOH); IR (KBr,  $\nu$  cm<sup>-1</sup>): 3410–3233 (4NH), 2200 (C≡N), 1678–1630 (2C=O). <sup>1</sup>H NMR (DMSO-*d*<sub>6</sub>):  $\delta$  3.78 (s, 3H, OCH<sub>3</sub>), 4.81 (s, 2H, CH<sub>2</sub>), 7.19–7.24 (m, 2H, Ar-H), 7.25–7.28 (m, 3H, Ar-H), 7.34–7.37 (m, 3H, Ar-H), 7.47–7.51 (m, 3H, Ar-H), 7.62 (d, *J* = 8.7 Hz, 2H, Ar-H), 8.63 (s, 1H, NH, D<sub>2</sub>O exchangeable), 9.21 (s, 1H, NH, D<sub>2</sub>O exchangeable), 10.62 (s, 1H, NH, D<sub>2</sub>O exchangeable), 11.22 (s, 1H, NH, D<sub>2</sub>O exchangeable). <sup>13</sup>C NMR (DMSO-*d*<sub>6</sub>):  $\delta$  54.8 (CH<sub>2</sub>), 55.9 (OCH<sub>3</sub>), 68.1, 98.1, 111.4 (C≡N), 115.1, 121.0, 123.0, 129.2, 131.3, 131.6, 136.4, 136.9, 137.9, 149.2, 151.4, 152.2, 156.2, 164.1, 165.8, 166.8. MS (*m/z*, %): 532 (M + 1<sup>+</sup>, 18.45), 531 (M<sup>+</sup>, 21.55), 449 (100). Anal. Calcd. for C<sub>27</sub>H<sub>22</sub>ClN<sub>5</sub>O<sub>3</sub>S (531.01): C, 60.96; H, 4.17; N, 13.16; Found: C, 60.80; H, 4.30; N, 13.18.

**2.1.4.3. 4-[2-(4-Bromophenyl)aminoacetamido]-5-cyano-N-(4-methoxyphenyl)-2-phenylaminothiophene-3-carboxamide (6).** Yield 55% (0.32 g); mp 217–219 °C (EtOH); IR (KBr,  $\nu$  cm<sup>-1</sup>): 3412–3225 (4NH), 2202 (C≡N), 1670–1645 (2C=O). <sup>1</sup>H NMR (DMSO-*d*<sub>6</sub>):  $\delta$  3.87 (s, 3H, OCH<sub>3</sub>), 4.83 (s, 2H, CH<sub>2</sub>), 7.08–7.13 (m, 5H, Ar-H), 7.26–7.35 (m, 4H, Ar-H), 7.37–7.41 (m, 4H, Ar-H), 9.60 (s, 1H, NH, D<sub>2</sub>O exchangeable),

10.49 (s, 1H, NH, D<sub>2</sub>O exchangeable), 11.20 (s, 2H, 2NH, D<sub>2</sub>O exchangeable). <sup>13</sup>C NMR (DMSO-*d*<sub>6</sub>):  $\delta$  54.7 (CH<sub>2</sub>), 55.5 (OCH<sub>3</sub>), 67.8, 98.6, 111.2 (C≡N), 120.7, 120.8, 121.3, 126.5, 129.0, 131.4, 138.2, 138.3, 145.8, 148.8, 148.9, 152.1, 157.9, 164.3, 165.8, 166.5. MS (*m/z*, %): 576 (M + 1<sup>+</sup>, 19.45), 575 (M<sup>+</sup>, 21.45), 448 (100). Anal. Calcd. for C<sub>27</sub>H<sub>22</sub>BrN<sub>5</sub>O<sub>3</sub>S (575.06): C, 56.25; H, 3.85; N, 12.15; Found: C, 56.10; H, 4.10; N, 12.28.

**2.1.4.4. 5-Cyano-N-(4-methoxyphenyl)-2-phenylamino-4-[2-(4-methyl-phenyl)aminoacetamido]thiophene-3-carboxamide (7).** Yield 78% (0.40 g); mp 197–200 °C (DMF); IR (KBr,  $\nu$  cm<sup>-1</sup>): 3425–3240 (4NH), 2200 (C≡N), 1675–1635 (2C=O). <sup>1</sup>H NMR (DMSO-*d*<sub>6</sub>):  $\delta$  2.30 (s, 3H, CH<sub>3</sub>), 3.78 (s, 3H, OCH<sub>3</sub>), 4.81 (s, 2H, CH<sub>2</sub>), 7.19–7.24 (m, 4H, Ar-H), 7.25–7.28 (m, 3H, Ar-H), 7.34–7.37 (m, 2H, Ar-H), 7.47–7.51 (m, 2H, Ar-H), 7.62 (d, *J* = 8.7 Hz, 2H, Ar-H), 9.56 (s, 1H, NH, D<sub>2</sub>O exchangeable), 10.51 (s, 1H, NH, D<sub>2</sub>O exchangeable), 10.81 (s, 1H, NH, D<sub>2</sub>O exchangeable), 11.22 (s, 1H, NH, D<sub>2</sub>O exchangeable). <sup>13</sup>C NMR (DMSO-*d*<sub>6</sub>):  $\delta$  23.4 (CH<sub>3</sub>), 54.9 (CH<sub>2</sub>), 55.7 (OCH<sub>3</sub>), 68.3, 97.8, 111.2 (C≡N), 119.0, 122.9, 123.0, 129.1, 129.2, 131.3, 132.4, 136.1, 136.3, 149.1, 152.2, 156.2, 158.6, 164.1, 165.1, 166.7. Anal. Calcd. for C<sub>28</sub>H<sub>25</sub>N<sub>5</sub>O<sub>3</sub>S (511.17): C, 65.74; H, 4.93; N, 13.69; Found: C, 65.51; H, 4.80; N, 13.88.

**2.1.4.5. 5-Cyano-N-(4-methoxyphenyl)-4-[2-(4-hydroxyphenyl)aminoacetamido]-2-phenylaminothiophene-3-carboxamide (8).** Yield 72% (0.37 g); mp 212–215 °C (DMF); IR (KBr,  $\nu$  cm<sup>-1</sup>): 3435–3222 (OH, 4NH), 2204 (C≡N), 1672–1634 (2C=O). <sup>1</sup>H NMR (DMSO-*d*<sub>6</sub>):  $\delta$  3.87 (s, 3H, OCH<sub>3</sub>), 4.83 (s, 2H, CH<sub>2</sub>), 7.08–7.11 (m, 2H, Ar-H), 7.12–7.15 (m, 3H, Ar-H), 7.29–7.32 (m, 3H, Ar-H), 7.3–7.36 (m, 3H, Ar-H), 7.37–7.43 (m, 2H, Ar-H), 9.60 (s, 1H, NH, D<sub>2</sub>O exchangeable), 10.19 (s, 1H, OH, D<sub>2</sub>O exchangeable), 10.53 (s, 1H, NH, D<sub>2</sub>O exchangeable), 10.81 (s, 1H, NH, D<sub>2</sub>O exchangeable), 11.21 (s, 1H, NH, D<sub>2</sub>O exchangeable). <sup>13</sup>C NMR (DMSO-*d*<sub>6</sub>):  $\delta$  54.9 (CH<sub>2</sub>), 55.4 (OCH<sub>3</sub>), 67.8, 98.4, 111.1 (C≡N), 119.0, 120.7, 120.8, 121.3, 126.5, 129.0, 131.3, 138.6, 145.8, 148.8, 148.9, 152.1, 157.9, 164.8, 165.3, 166.6. Anal. Calcd. for C<sub>27</sub>H<sub>23</sub>N<sub>5</sub>O<sub>4</sub>S (513.57): C, 63.14; H, 4.51; N, 13.64; Found: C, 62.94; H, 4.63; N, 13.59.

**2.1.4.6. 5-Cyano-N-(4-methoxyphenyl)-4-[2-(4-methoxyphenyl)aminoacetamido]-2-phenylaminothiophene-3-carboxamide (9).** Yield 66% (0.35 g); mp 212–215 °C (DMF); IR (KBr,  $\nu$  cm<sup>-1</sup>): 3410–3225 (4NH), 2198 (C≡N), 1676–1638 (2C=O). <sup>1</sup>H NMR (DMSO-*d*<sub>6</sub>):  $\delta$  3.78 (s, 3H, OCH<sub>3</sub>), 3.80 (s, 3H, OCH<sub>3</sub>), 4.81 (s, 2H, CH<sub>2</sub>), 7.15–7.24 (m, 3H, Ar-H), 7.25–7.32 (m, 2H, Ar-H), 7.34–7.41 (m, 2H, Ar-H), 7.42–7.47 (m, 6H, Ar-H), 9.72 (s, 1H, NH, D<sub>2</sub>O exchangeable), 10.52 (s, 1H, NH, D<sub>2</sub>O exchangeable), 10.82 (s, 1H, NH, D<sub>2</sub>O exchangeable), 11.22 (s, 1H, NH, D<sub>2</sub>O exchangeable). <sup>13</sup>C NMR (DMSO-*d*<sub>6</sub>):  $\delta$  54.8 (CH<sub>2</sub>), 55.1 (OCH<sub>3</sub>), 55.4 (OCH<sub>3</sub>), 67.8, 98.4, 111.1 (C≡N), 120.6, 122.8, 122.9, 126.4, 129.2, 131.2, 133.9, 138.1, 142.7, 155.2, 155.7, 156.3, 164.4, 165.3, 166.7. Anal. Calcd. for C<sub>28</sub>H<sub>25</sub>N<sub>5</sub>O<sub>4</sub>S (527.16): C, 63.74; H, 4.78; N, 13.27; Found: C, 63.50; H, 4.70; N, 13.48.

**2.1.4.7. 5-Cyano-N-(4-methoxyphenyl)-4-[2-(4-nitrophenyl)aminoacetamido]-2-phenylaminothiophene-3-carboxamide (10).** Yield 61% (0.33 g); mp 188–191 °C (EtOH); IR (KBr,  $\nu$  cm<sup>-1</sup>): 3414–3230 (4NH), 2200 (C≡N), 1678–1635 (2C=O). <sup>1</sup>H NMR (DMSO-*d*<sub>6</sub>):  $\delta$  3.79 (s, 3H, OCH<sub>3</sub>), 4.78 (s, 2H, CH<sub>2</sub>), 7.05–7.14 (m, 2H, Ar-H), 7.17–7.21 (m, 2H, Ar-H), 7.23–7.32 (m, 3H, Ar-H), 7.39–7.51 (m, 4H, Ar-H), 7.54–8.05 (m, 2H, Ar-H), 9.51 (s, 1H, NH, D<sub>2</sub>O exchangeable), 10.75 (s, 1H, NH, D<sub>2</sub>O exchangeable), 11.24 (s, 2H, 2NH, D<sub>2</sub>O exchangeable). <sup>13</sup>C NMR (DMSO-*d*<sub>6</sub>):  $\delta$  54.9 (CH<sub>2</sub>), 55.3 (OCH<sub>3</sub>), 67.8, 97.8, 111.0 (C≡N), 120.7, 121.3, 126.5, 129.0, 131.3, 131.4, 138.2, 138.6,

145.8, 148.8, 148.9, 152.1, 158.0, 164.6, 165.6, 166.9. MS ( $m/z$ , %): 543 ( $M+1^+$ , 18.15), 542 ( $M^+$ , 30.46), 364 (100). Anal. Calcd. for  $C_{27}H_{22}N_6O_5S$  (542.14): C, 59.77; H, 4.09; N, 15.49; Found: C, 59.80; H, 4.30; N, 15.68.

**2.1.4.8. 5-Cyano-N-(4-methoxyphenyl)-4-[2-(2-chlorophenyl) aminoacetamido]-2-phenylaminothiophene-3-carboxamide (11).** Yield, 66% (0.35 g); mp 156–158 °C (DMF); IR (KBr,  $\nu$   $cm^{-1}$ ): 3415–3234 (4NH), 2201 ( $C\equiv N$ ), 1678–1635 ( $C=O$ ).  $^1H$  NMR (DMSO- $d_6$ ):  $\delta$  3.76 (s, 3H,  $OCH_3$ ), 4.86 (s, 2H,  $CH_2$ ), 7.01–7.13 (m, 3H, Ar-H), 7.15–7.25 (m, 2H, Ar-H), 7.34–7.38 (m, 4H, Ar-H), 7.41–7.48 (m, 2H, Ar-H), 7.78 (d,  $J=7.2$  Hz, 2H, Ar-H), 8.62 (s, 1H, NH,  $D_2O$  exchangeable), 9.21 (s, 1H, NH,  $D_2O$  exchangeable), 10.18 (s, 1H, NH,  $D_2O$  exchangeable), 11.34 (s, 1H, NH,  $D_2O$  exchangeable).  $^{13}C$  NMR (DMSO- $d_6$ ):  $\delta$  54.8 ( $CH_2$ ), 55.5 ( $OCH_3$ ), 68.7, 99.1, 111.3 ( $C\equiv N$ ), 120.7, 120.8, 121.3, 126.5, 129.0, 131.3, 131.4, 138.2, 138.6, 145.8, 148.8, 148.9, 152.1, 157.9, 164.0, 165.8, 166.1. Anal. Calcd. for  $C_{27}H_{22}ClN_5O_3S$  (532.01): C, 60.96; H, 4.17; N, 13.16; Found: C, 60.70; H, 4.20; N, 13.30.

**2.1.4.9. 5-Cyano-N-(4-methoxyphenyl)-4-[2-(2-nitrophenyl)aminoacetamido]-2-phenylaminothiophene-3-carboxamide (12).** Yield 59% (0.32 g); mp 167–168 °C; IR (KBr,  $\nu$   $cm^{-1}$ ): 3430–3224 (4NH), 2203 ( $C\equiv N$ ), 1672–1639 ( $2C=O$ ).  $^1H$  NMR (DMSO- $d_6$ ):  $\delta$  3.84 (s, 3H,  $OCH_3$ ), 4.75 (s, 2H,  $CH_2$ ), 7.06–7.18 (m, 4H, Ar-H), 7.20–7.46 (m, 5H, Ar-H), 7.47–7.77 (m, 2H, Ar-H), 8.01–8.03 (m, 2H, Ar-H), 9.67 (s, 1H, NH,  $D_2O$  exchangeable), 10.57 (s, 1H, NH,  $D_2O$  exchangeable), 10.87 (s, 1H, NH,  $D_2O$  exchangeable), 11.18 (s, 1H, NH,  $D_2O$  exchangeable).  $^{13}C$  NMR (DMSO- $d_6$ ):  $\delta$  54.9 ( $CH_2$ ), 55.9 ( $OCH_3$ ), 68.2, 98.8, 111.9 ( $C\equiv N$ ), 120.7, 120.8, 121.3, 126.5, 129.0, 131.3, 131.4, 138.2, 138.6, 145.9, 148.8, 148.9, 152.2, 157.9, 164.9, 165.4, 166.9. Anal. Calcd. for  $C_{27}H_{22}N_6O_5S$  (542.57): C, 59.77; H, 4.09; N, 15.49; Found: C, 59.50; H, 4.30; N, 15.28.

**2.1.4.10. 5-Cyano-N-(4-methoxyphenyl)-4-[2-(3,4-dimethoxyphenyl) aminoacetamido]-2-phenylaminothiophene-3-carboxamide (13).** Yield, 52% (0.29 g); mp 167–168 °C; IR (KBr,  $\nu$   $cm^{-1}$ ): 3425–3214 (4NH), 2209 ( $C\equiv N$ ), 1672–1633 ( $2C=O$ ).  $^1H$  NMR (DMSO- $d_6$ ):  $\delta$  3.65 (s, 3H,  $OCH_3$ ), 3.71 (s, 3H,  $OCH_3$ ), 3.75 (s, 3H,  $OCH_3$ ), 4.83 (s, 2H,  $CH_2$ ), 7.04–7.07 (m, 2H, Ar-H), 7.18–7.23 (m, 3H, Ar-H), 7.33–7.40 (m, 3H, Ar-H), 7.45–7.47 (m, 4H, Ar-H), 9.59 (s, 1H, NH,  $D_2O$  exchangeable), 10.53 (s, 1H, NH,  $D_2O$  exchangeable), 10.81 (s, 1H, NH,  $D_2O$  exchangeable), 11.29 (s, 1H, NH,  $D_2O$  exchangeable).  $^{13}C$  NMR (DMSO- $d_6$ ):  $\delta$  54.9 ( $CH_2$ ), 55.1 ( $OCH_3$ ), 55.9 ( $OCH_3$ ), 68.2, 98.8, 111.8 ( $C\equiv N$ ), 115.1, 121.0, 123.0, 129.3, 131.4, 131.7, 136.4, 137.0, 138.0, 151.4, 152.2, 156.2, 164.4, 165.2, 166.4. Anal. Calcd. for  $C_{29}H_{27}N_5O_5S$  (557.62): C, 62.46; H, 4.88; N, 12.56; Found: C, 62.27; H, 5.03; N, 12.50.

#### 2.1.5. Procedure for synthesis of ethyl -3-acetamido-4-(4-methoxyphenylcarbamoyl)-5-phenylaminothiophene-2-carboxylate (14)

To a stirred solution of ethyl 3-amino-4-(4-methoxyphenylcarbamoyl)-5-phenylaminothiophene-2-carboxylate **2b** (0.41 g, 0.001 mol) in *n*-butanol (5 ml), acetyl chloride (0.08 g, 0.001 mol) was added drop-wise with cooling and the reaction mixture was irradiated at 140 °C for 5 min in the microwave oven. After cooling to room temperature, the solid produced was collected and treated with sodium carbonate solution (10%, 20 ml) then filtered, washed with water, dried and recrystallized from the ethanol to afford crystals of ethyl 3-acetamido-4,5-disubstitutedthiophene-2-carboxylate **14**. Yield 71% (0.32 g); mp 293–295 °C; IR (KBr,  $\nu$   $cm^{-1}$ ): 3429–3263 (3NH), 1682–1641 ( $3C=O$ );  $^1H$  NMR (DMSO- $d_6$ ):  $\delta$  1.25 (t,

$J=6.9$  Hz, 3H,  $OCH_2CH_3$ ), 2.26 (s, 3H,  $COCH_3$ ), 3.56 (s, 3H,  $OCH_3$ ), 4.23 (q,  $J=6.9$  Hz, 2H,  $OCH_2CH_3$ ), 7.10–7.13 (m, 3H, Ar-H), 7.36–7.39 (m, 4H, Ar-H), 7.41–7.49 (m, 2H, Ar-H), 9.56 (s, 1H, NH,  $D_2O$  exchangeable), 9.81 (s, 1H, NH,  $D_2O$  exchangeable), 10.08 (s, 1H, NH,  $D_2O$  exchangeable).  $^{13}C$  NMR (DMSO- $d_6$ ):  $\delta$  14.2 ( $OCH_2CH_3$ ), 22.9 ( $COCH_3$ ), 55.9 ( $OCH_3$ ), 60.9 ( $OCH_2CH_3$ ), 99.2, 114.8, 119.6, 123.0, 128.8, 131.3, 136.9, 138.5, 151.4, 152.2, 158.2, 160.4, 165.3, 166.7, 170.1. MS  $m/z$ : 454 ( $M+1^+$ , 8.76), 453 ( $M^+$ , 13.23), 287 (100). Anal. Calcd. for  $C_{23}H_{23}N_3O_5S$  (453.51): C, 60.91; H, 5.11; N, 9.27. Found: C, 61.13; H, 4.98; N, 9.34.

#### 2.1.6. Procedure for synthesis of 4-acetamido-5-hydrazinocarbonyl-N-(4-methoxyphenyl)-2-phenylaminothiophene-3-carboxamide (15)

A mixture of ethyl 3-acetamido-4-(4-methoxyphenylcarbamoyl)-5-phenylaminothiophene-2-carboxylate **14** (0.45 g, 0.001 mol) and hydrazine hydrate (99%, 0.001 mol) in *n*-butanol (5 ml) was heated at 150 °C for 5 min in the microwave oven. After cooling to room temperature, the separated solid was filtered, washed with hot ethanol, dried and recrystallized from acetic acid to yield hydrazide derivative **15**. Yield, 84% (0.37 g); mp > 300 °C; IR (KBr,  $\nu$   $cm^{-1}$ ): 3340–3275 (4NH,  $NH_2$ ), 1673–1632 ( $3C=O$ );  $^1H$  NMR (DMSO- $d_6$ ):  $\delta$  2.27 (s, 3H,  $COCH_3$ ), 3.67 (s, 3H,  $OCH_3$ ), 7.11–7.21 (m, 2H, Ar-H), 7.39–7.45 (m, 3H, Ar-H), 7.48–7.54 (m, 2H, Ar-H), 7.84 (d,  $J=8.4$  Hz, 2H, Ar-H), 9.60 (s, 2H,  $NH_2$ ,  $D_2O$  exchangeable), 9.64 (s, 1H, NH,  $D_2O$  exchangeable), 10.31 (s, 1H, NH,  $D_2O$  exchangeable), 11.40 (s, 1H, NH,  $D_2O$  exchangeable).  $^{13}C$  NMR (DMSO- $d_6$ ):  $\delta$  22.8 ( $COCH_3$ ), 55.9 ( $OCH_3$ ), 99.2, 114.8, 119.0, 122.9, 129.2, 131.3, 132.4, 136.0, 136.9, 149.1, 156.2, 158.6, 164.4, 165.3, 166.7. MS  $m/z$ : 440 ( $M+1^+$ , 0.49), 439 ( $M^+$ , 2.75), 267 (100). Anal. Calcd. for  $C_{21}H_{21}N_5O_4S$  (439.49): C, 57.39; H, 4.82; N, 15.94. Found: C, 57.62; H, 5.01; N, 15.72.

#### 2.1.7. General procedure for synthesis of 4-acetamido-5-(2-arylidenehydrazinocarbonyl)-N-(4-methoxyphenyl)-2-phenylaminothiophene-3-carboxamides 16–23

To a well stirred solution of hydrazide **15** (0.44 g, 0.001 mol) in glacial acetic acid (5 ml), the appropriate aromatic aldehyde (0.001 mol) was added. The reaction mixture was irradiated at 100 °C in the microwave oven for 15 min and set aside to cool at room temperature. The separated solid was filtered, washed with hot ethanol and recrystallized from the proper solvent to afford 5-(2-arylidenehydrazinocarbonyl)thiophene-3-carboxamides **16–23**.

##### 2.1.7.1. 4-Acetamido-5-(2-benzylidenehydrazinocarbonyl)-N-(4-methoxyphenyl)-2-phenylaminothiophene-3-carboxamide (16).

Yield, 59% (0.31 g); mp 256–258 °C (EtOH); IR (KBr,  $\nu$   $cm^{-1}$ ): 3444–3212 (4NH), 1668–1630 ( $3C=O$ ), 1587 ( $C=N$ );  $^1H$  NMR (DMSO- $d_6$ ):  $\delta$  2.30 (s, 3H,  $COCH_3$ ), 3.62 (s, 3H,  $OCH_3$ ), 7.18–7.24 (m, 6H, Ar-H), 7.48–7.50 (m, 5H, Ar-H), 7.57–7.60 (m, 3H, Ar-H), 8.39 (s, 1H,  $CH=N$ ), 8.64 (s, 1H, NH,  $D_2O$  exchangeable), 9.76 (s, 1H, NH,  $D_2O$  exchangeable), 11.43 (s, 1H, NH,  $D_2O$  exchangeable), 11.47 (s, 1H, NH,  $D_2O$  exchangeable);  $^{13}C$  NMR (DMSO- $d_6$ ):  $\delta$  22.9 ( $COCH_3$ ), 55.9 ( $OCH_3$ ), 99.2, 114.1, 120.7, 120.8, 121.3, 126.5, 129.0, 131.3, 131.4, 138.2, 138.6, 145.8, 148.8, 148.9, 152.1, 157.1 ( $CH=N$ ), 164.0, 168.7, 168.8, 170.4. MS  $m/z$ : 528 ( $M+1^+$ , 18.38), 527 ( $M^+$ , 22.62), 348 (100). Anal. Calcd. for  $C_{28}H_{25}N_5O_4S$  (527.59): C, 63.74; H, 4.78; N, 13.27; Found: C, 63.55; H, 4.58; N, 13.42.

##### 2.1.7.2. 4-Acetamido-5-[2-(4-chlorobenzylidene)hydrazinocarbonyl]-N-(4-methoxyphenyl)-2-phenylaminothiophene-3-carboxamide (17).

Yield, 61% (0.34 g); mp 234–244 °C (PrOH); IR (KBr,  $\nu$   $cm^{-1}$ ):

3338–3213 (4NH), 1650–1643 (3C=O), 1590 (C=N);  $^1\text{H}$  NMR (DMSO- $d_6$ ):  $\delta$  2.32 (s, 3H, COCH<sub>3</sub>), 3.50 (s, 3H, OCH<sub>3</sub>), 7.07–7.14 (m, 3H, Ar-H), 7.28–7.36 (m, 2H, Ar-H), 7.38–7.48 (m, 6H, Ar-H), 7.59 (d,  $J$ =8.1 Hz, 2H, Ar-H), 8.41 (s, 1H, CH=N), 8.63 (s, 1H, NH, D<sub>2</sub>O exchangeable), 9.76 (s, 1H, NH, D<sub>2</sub>O exchangeable), 9.84 (s, 1H, NH, D<sub>2</sub>O exchangeable), 10.10 (s, 1H, NH, D<sub>2</sub>O exchangeable);  $^{13}\text{C}$  NMR (DMSO- $d_6$ ):  $\delta$  22.0 (COCH<sub>3</sub>), 56.8 (OCH<sub>3</sub>), 99.5, 114.2, 120.7, 120.8, 121.3, 126.5, 129.0, 131.3, 131.4, 138.2, 138.6, 145.8, 148.8, 148.9, 152.1, 157.9 (CH=N), 164.8, 168.1, 168.2, 170.1. MS  $m/z$  (%): 563 ( $M+2^+$ , 3.83), 561 ( $M^+$ , 9.09), 541 (100). Anal. Calcd. for C<sub>28</sub>H<sub>24</sub>ClN<sub>5</sub>O<sub>4</sub>S (562.04): C, 59.84; H, 4.30; N, 12.46; Found: C, 59.72; H, 4.68; N, 12.59.

**2.1.7.3. 4-Acetamido-5-[2-(4-bromobenzylidene)hydrazinocarbonyl]-N-(4-methoxyphenyl)-2-phenylaminothiophene-3-carboxamide (18).** Yield, 84% (0.51 g); mp 247–250 °C (EtOH); IR (KBr,  $\nu$  cm<sup>-1</sup>): 3343–3210 (4NH), 1650–1634 (3C=O), 1590 (C=N);  $^1\text{H}$  NMR (DMSO- $d_6$ ):  $\delta$  2.24 (s, 3H, COCH<sub>3</sub>), 3.62 (s, 3H, OCH<sub>3</sub>), 7.05–7.18 (m, 6H, Ar-H), 7.31–7.41 (m, 4H, Ar-H), 7.49–7.52 (m, 3H, Ar-H), 8.34 (s, 1H, CH=N), 8.59 (s, 1H, NH, D<sub>2</sub>O exchangeable), 9.49 (s, 1H, NH, D<sub>2</sub>O exchangeable), 9.57 (s, 1H, NH, D<sub>2</sub>O exchangeable), 11.28 (s, 1H, NH, D<sub>2</sub>O exchangeable);  $^{13}\text{C}$  NMR (DMSO- $d_6$ ):  $\delta$  23.2 (COCH<sub>3</sub>), 55.11 (OCH<sub>3</sub>), 99.7, 114.9, 120.7, 120.8, 121.3, 126.5, 129.0, 131.3, 131.4, 138.2, 138.6, 145.8, 148.8, 148.9, 152.1, 157.9 (CH=N), 164.6, 168.2, 168.3, 170.3. Anal. Calcd. for: C<sub>28</sub>H<sub>24</sub>BrN<sub>5</sub>O<sub>4</sub>S (606.49), C, 55.45; H, 3.99; N, 11.55; Found: C, 55.27; H, 3.90; N, 11.35.

**2.1.7.4. 4-Acetamido-5-[2-(4-methylbenzylidene)hydrazinocarbonyl]-N-(4-methoxyphenyl)-2-phenylaminothiophene-3-carboxamide (19).** Yield, 78% (0.42 g); mp 180–183 °C (DMF); IR (KBr,  $\nu$  cm<sup>-1</sup>): 3335–3218 (4NH), 1668–1633 (3C=O), 1593 (C=N);  $^1\text{H}$  NMR (DMSO- $d_6$ ):  $\delta$  2.05 (s, 3H, CH<sub>3</sub>), 2.37 (s, 3H, COCH<sub>3</sub>), 3.68 (s, 3H, OCH<sub>3</sub>), 7.07–7.13 (m, 5H, Ar-H), 7.29–7.41 (m, 6H, Ar-H), 7.59 (d,  $J$ =8.4 Hz, 2H, Ar-H), 8.41 (s, 1H, CH=N), 9.61 (s, 1H, NH, D<sub>2</sub>O exchangeable), 9.68 (s, 1H, NH, D<sub>2</sub>O exchangeable), 9.86 (s, 1H, NH, D<sub>2</sub>O exchangeable), 11.28 (s, 1H, NH, D<sub>2</sub>O exchangeable);  $^{13}\text{C}$  NMR (DMSO- $d_6$ ):  $\delta$  22.9 (COCH<sub>3</sub>), 24.3 (CH<sub>3</sub>), 55.6 (OCH<sub>3</sub>), 99.1, 114.4, 120.7, 120.8, 121.3, 126.5, 129.0, 131.3, 131.4, 138.2, 138.6, 145.8, 148.8, 148.9, 152.1, 157.9 (CH=N), 164.4, 168.1, 168.2, 170.8. MS  $m/z$ : 542 ( $M+1^+$ , 17.34), 541 ( $M^+$ , 24.17), 348 (100). Anal. Calcd. for C<sub>29</sub>H<sub>27</sub>N<sub>5</sub>O<sub>4</sub>S (541.62): C, 64.31; H, 5.02; N, 12.93; Found: C, 64.45; H, 5.11; N, 13.02.

**2.1.7.5. 4-Acetamido-5-[2-(4-methoxybenzylidene)hydrazinocarbonyl]-N-(4-methoxyphenyl)-2-(phenylamino)thiophene-3-carboxamide (20).** Yield, 66% (0.37 g); mp 259–661 °C (DMF); IR (KBr,  $\nu$  cm<sup>-1</sup>): 3443–3225 (4NH), 1691–1640 (3C=O), 1592 (C=N);  $^1\text{H}$  NMR (DMSO- $d_6$ ):  $\delta$  2.22 (s, 3H, COCH<sub>3</sub>), 3.78 (s, 3H, OCH<sub>3</sub>), 3.82 (s, 3H, OCH<sub>3</sub>), 7.07–7.13 (m, 3H, Ar-H), 7.25–7.27 (m, 2H, Ar-H), 7.36–7.41 (m, 4H, Ar-H), 7.57 (d,  $J$ =8.4 Hz, 2H, Ar-H), 8.13 (d,  $J$ =8.4 Hz, 2H, Ar-H), 8.39 (s, 1H, CH=N), 9.54 (s, 1H, NH, D<sub>2</sub>O exchangeable), 9.82 (s, 1H, NH, D<sub>2</sub>O exchangeable), 10.28 (s, 1H, NH, D<sub>2</sub>O exchangeable), 11.29 (s, 1H, NH, D<sub>2</sub>O exchangeable);  $^{13}\text{C}$  NMR (DMSO- $d_6$ ):  $\delta$  22.3 (COCH<sub>3</sub>), 54.2 (OCH<sub>3</sub>), 55.3 (OCH<sub>3</sub>), 99.6, 114.2, 121.0, 123.0, 129.2, 131.3, 131.6, 136.4, 136.9, 137.9, 151.4, 152.2, 156.2 (CH=N), 163.1, 164.6, 168.1, 168.2, 170.4. Anal. Calcd. for C<sub>29</sub>H<sub>27</sub>N<sub>5</sub>O<sub>5</sub>S (557.62): C, 62.46; H, 4.88; N, 12.56; Found: C, 62.53; H, 4.67; N, 12.72.

**2.1.7.6. 4-Acetamido-5-[2-(3-hydroxy-4-methoxybenzylidene)hydrazinocarbonyl]-N-(4-methoxyphenyl)-2-phenylaminothiophene-3-carboxamide (21).** Yield, 63% (0.36 g); mp 292–295 °C (PrOH); IR (KBr,  $\nu$

cm<sup>-1</sup>): 3440–3132 (OH, 4NH), 1667–1646 (3C=O), 1592 (C=N);  $^1\text{H}$  NMR (DMSO- $d_6$ ):  $\delta$  2.29 (s, 3H, COCH<sub>3</sub>), 3.58 (s, 3H, OCH<sub>3</sub>), 3.61 (s, 3H, OCH<sub>3</sub>), 5.38 (s, 1H, OH, D<sub>2</sub>O exchangeable), 7.12–7.21 (m, 3H, Ar-H), 7.35–7.37 (m, 3H, Ar-H), 7.41–7.55 (m, 6H, Ar-H), 8.31 (s, 1H, CH=N), 8.61 (s, 1H, NH, D<sub>2</sub>O exchangeable), 9.64 (s, 1H, NH, D<sub>2</sub>O exchangeable), 9.72 (s, 1H, NH, D<sub>2</sub>O exchangeable), 11.23 (s, 1H, NH, D<sub>2</sub>O exchangeable);  $^{13}\text{C}$  NMR (DMSO- $d_6$ ):  $\delta$  22.5 (COCH<sub>3</sub>), 56.1 (OCH<sub>3</sub>), 56.2 (OCH<sub>3</sub>), 99.5, 119.0, 122.9, 123.0, 129.2, 129.3, 131.3, 132.4, 136.0, 136.2, 136.4, 136.9, 149.1, 152.3, 156.2 (CH=N), 158.7, 164.1, 168.4, 168.5, 170.2. MS  $m/z$ : 574 ( $M+1^+$ , 11.61), 573 ( $M^+$ , 15.45), 307 (100). Anal. Calcd. for C<sub>29</sub>H<sub>27</sub>N<sub>5</sub>O<sub>6</sub>S (573.62): C, 60.72; H, 4.74; N, 12.21; Found: C, 60.86; H, 4.66; N, 12.48.

**2.1.7.7. 4-Acetamido-5-[2-(3,4-dimethoxybenzylidene)hydrazinocarbonyl]-N-(4-methoxyphenyl)-2-phenylaminothiophene-3-carboxamide (22).** Yield, 63% (0.37 g); mp 233–235 °C (PrOH); IR (KBr,  $\nu$  cm<sup>-1</sup>): 3411–3108 (4NH), 1667–1640 (3C=O), 1592 (C=N);  $^1\text{H}$  NMR (DMSO- $d_6$ ):  $\delta$  2.24 (s, 3H, COCH<sub>3</sub>), 3.61 (s, 3H, OCH<sub>3</sub>), 3.66 (s, 3H, OCH<sub>3</sub>), 3.75 (s, 3H, OCH<sub>3</sub>), 7.10–7.23 (m, 5H, Ar-H), 7.34–7.44 (m, 7H, Ar-H), 8.39 (s, 1H, CH=N), 8.59 (s, 1H, NH, D<sub>2</sub>O exchangeable), 9.86 (s, 1H, NH, D<sub>2</sub>O exchangeable), 10.63 (s, 1H, NH, D<sub>2</sub>O exchangeable), 11.23 (s, 1H, NH, D<sub>2</sub>O exchangeable);  $^{13}\text{C}$  NMR (DMSO- $d_6$ ):  $\delta$  23.1 (COCH<sub>3</sub>), 55.8 (OCH<sub>3</sub>), 55.9 (OCH<sub>3</sub>), 56.0 (OCH<sub>3</sub>), 99.4, 114.0, 120.7, 120.8, 121.3, 126.5, 129.0, 131.3, 131.4, 138.2, 138.6, 145.9, 148.8, 148.9, 152.2, 157.9 (CH=N), 164.1, 168.3, 168.4, 170.1. MS  $m/z$ : 588 ( $M+1^+$ , 2.19), 587 ( $M^+$ , 6.21), 347 (100). Anal. Calcd. for C<sub>30</sub>H<sub>29</sub>N<sub>5</sub>O<sub>6</sub>S (587.65): C, 61.32; H, 4.97; N, 12.92; Found: C, 60.98; H, 4.78; N, 12.70.

**2.1.7.8. 4-Acetamido-N-(p-methoxyphenyl)-2-phenylamino-5-[2-(3,4,5-trimethoxybenzylidene)hydrazinocarbonyl]thiophene-3-carboxamide (23).** Yield, 61% (0.38 g); mp 283–285 °C (PrOH); IR (KBr,  $\nu$  cm<sup>-1</sup>): 3411–3108 (4NH), 1667–1646 (3C=O), 1592 (C=N);  $^1\text{H}$  NMR (DMSO- $d_6$ ):  $\delta$  2.23 (s, 3H, COCH<sub>3</sub>), 3.76 (s, 3H, OCH<sub>3</sub>), 3.79 (s, 3H, OCH<sub>3</sub>), 3.82 (s, 3H, OCH<sub>3</sub>), 3.83 (s, 3H, OCH<sub>3</sub>), 7.16–7.23 (m, 6H, Ar-H), 7.32–7.53 (m, 5H, Ar-H), 8.39 (s, 1H, CH=N), 8.69 (s, 2H, 2NH, D<sub>2</sub>O exchangeable), 9.63 (s, 1H, NH, D<sub>2</sub>O exchangeable), 10.29 (s, 1H, NH, D<sub>2</sub>O exchangeable);  $^{13}\text{C}$  NMR (DMSO- $d_6$ ):  $\delta$  23.2 (COCH<sub>3</sub>), 55.7 (OCH<sub>3</sub>), 55.8 (OCH<sub>3</sub>), 55.9 (OCH<sub>3</sub>), 99.2, 107.1, 120.6, 122.8, 122.9, 126.4, 129.2, 131.2, 133.9, 138.1, 142.8, 155.2, 155.8, 156.4 (CH=N), 164.2, 168.6, 168.6, 170.6. MS  $m/z$ : 618 ( $M+1^+$ , 23.95), 617 ( $M^+$ , 26.12), 502 (100). Anal. Calcd. for C<sub>31</sub>H<sub>31</sub>N<sub>5</sub>O<sub>7</sub>S (617.67): C, 60.28; H, 5.06; N, 11.34; Found: C, 60.33; H, 5.18; N, 11.10.

## 2.2. Biological screening

### 2.2.1. Measurement of potential cytotoxic activity:

The cytotoxic activity of all the newly synthesized compounds was measured *in vitro* on HepG-2 and HCT-116 cell lines with Sulforhodamine-B stain (SRB) according to the reported procedure<sup>43</sup>. Sorafenib was used as reference standard. Cells were seeded in 96-well microtiter plates at a concentration of  $5 \times 10^4$ – $10^5$  cells/well in a fresh medium and left to attach to the plates for 24 h before treatment with the tested compounds. Compounds were dissolved in dimethylsulfoxide (DMSO) and diluted with saline to the appropriate volume. After 24 h, cells were incubated with the appropriate concentration ranges of compounds (0.001, 0.01, 0.1, 1.0, 10, and 100  $\mu\text{M}$ ), the wells were diluted to 200  $\mu\text{L}$  with fresh medium and incubation was continued for 48 h. Control cells were treated with vehicle alone. Four wells were used for each drug concentration. After 48 h incubation, the cells were fixed with 50  $\mu\text{L}$  cold 50% trichloroacetic acid



for 1 h at 4 °C, washed 5 times with distilled water and then stained for 30 min. at room temperature with 50  $\mu$ L 0.4% SRB dissolved in 1% acetic acid. The wells were then washed 4 times with 1% acetic acid. The plates were air-dried and the dye was solubilized with 100  $\mu$ L/well of 10 mM Tris base (PH 10.5) for 5 min on a shaker (Orbital shaker OS 20, Boeco, Germany) at 1600 rpm. The optical density (OD) of each well was measured spectrophotometrically at 564 nm with an enzyme-linked immunosorbent assay (ELISA) microplate reader (Meter tech.  $\Sigma$  960, USA). The percentage of cell survival was calculated as follows: Survival fraction = OD (treated cells)/OD (control cells). The relation between surviving fraction and compound concentration was plotted and IC<sub>50</sub> [the concentration required for 50% inhibition of cell viability] was calculated for each test compound. Experiment was repeated three times for each concentration.

### 2.2.2. DNA-flow cytometry cell cycle analysis for compounds 5 and 21 on HepG-2 cells:

HepG-2 cells were treated with compounds **5** and **21** at their IC<sub>50</sub> values for 24 h. After treatment, cells were washed twice with ice-cold phosphate buffer saline (PBS), collected by centrifugation, and fixed in ice-cold 70% (v/v) ethanol, washed with PBS, re-suspended with 0.1 mg/mL RNase, stained with 40 mg/mL propidium iodide (PI), and analyzed by flow cytometry using FACS Calibur (Becton Dickinson)<sup>39</sup>. The cell cycle distributions were calculated using Cell-Quest software (Becton Dickinson). Exposure of HepG-2 cells to compounds **5** and **21** resulted in an interference with the normal cell cycle distribution as indicated in the text.

### 2.2.3. In vitro ELISA immunoassay measurement of apoptotic markers for the effect for compounds 5 and 21 on HepG-2 cells (P53, bax, bcl-2, caspase-3/7)

**2.2.3.1. Materials.** The levels of Bax, Bcl-2, caspase-3 and -7 were assessed using ELISA immunoassay. Kits were purchased from the indicated suppliers. DRG® Human Bax. ELISA (EIA-4487) Marburg, Germany. Bcl-2 ELISA Kit Invitrogen Corporation 1600 Faraday Avenue Carlsbad. Caspase-3, Invitrogen EIA kit Human (active) KHO1091 Invitrogen Corporation 1600 Faraday Avenue Carlsbad. Cloud clone caspase-7 (Active) eiakit, Cloud clone, Houston, USA. Procedures of the colorimetric kits were performed according to the manufacturer's instructions.

**2.2.3.2. Methodology.** The main principle of sandwich ELISA is the quantification of a specific protein through its containment in a sandwich of specific antibodies conjugated to the colorimetric TMB substrate, whose intensity is proportional to the protein quantity and is measured spectrophotometrically. The cell lysate was diluted 10 times, and 100  $\mu$ L (50 mg protein) was added to the wells of separate micro titer plates for the ELISA kits that were precoated with primary antibodies specific to Bax, Bcl-2, caspase-3 or caspase-7. A secondary biotin-linked antibody specific to the protein captured by the primary antibody was added to bind the captured protein, forming a "sandwich" of specific antibodies around the desired protein in the cell lysate. The streptavidin-HRP complex was then used to bind the biotin-linked secondary antibody through its streptavidin portion. The HRP domain reacted with the added TMB substrate, forming a colored product that was measured at 450 nm by a plate reader (ChroMate-4300, FL, USA) after the reaction was terminated by the addition of stop solution.

### 2.2.4. In vitro $\beta$ -tubulin polymerization inhibition assay for compounds 5 and 21

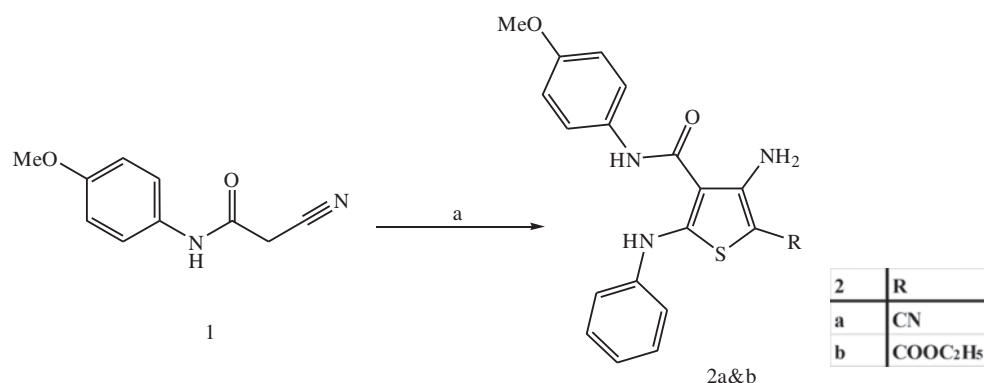
**2.2.4.1. Materials.** Enzyme linked immunosorbent assay (ELISA) was performed with human  $\beta$ -tubulin assay kit (SEB870HU) purchased from Cloud-Clone Corp. US. Procedures were performed according to manufacturer's instructions<sup>44</sup>.

**2.2.4.2. Methodology.** HepG-2 cell line was obtained from American Type Culture Collection, they were cultured using DMEM (Invitrogen/Life Technologies) supplemented with 10% FBS (Hyclone), 10 mg/mL of insulin (Sigma), and 1% penicillin-streptomycin. Plate cells (cells density 1.2–1.8  $\times$  10,000 cells/well) in a volume of 100 ml complete growth medium and 100 ml of the tested compound at its IC<sub>50</sub> per well in a 96-well plate for 18–24 h before the enzyme assay for  $\beta$ -TUB. The microtiter plate provided in this kit has been pre-coated with an antibody specific to  $\beta$ -TUB. Standards or samples are then added to the appropriate microtiter plate wells with a biotin-conjugated antibody specific to  $\beta$ -TUB. Next, Avidin conjugated to Horseradish Peroxidase (HRP) is added to each microplate well and incubated. After TMB substrate solution is added, only those wells that contain  $\beta$ -TUB, biotin-conjugated antibody and enzyme-conjugated Avidin will exhibit a change in color. The enzyme-substrate reaction is terminated by the addition of sulfuric acid solution and the color change is measured spectrophotometrically at a wavelength of 50 nm  $\pm$  10 nm. The concentration of  $\beta$ -TUB in the samples is then determined by comparing the O.D. of the samples to the standard curve. The data were compared with colchicine as standard  $\beta$ -TUB polymerization inhibitor. Each experiment was repeated three times.

### 2.2.5. In vitro vascular endothelial growth factor receptor-2 (VEGFR-2) enzyme assay for

**2.2.5.1. Materials.** Enzyme linked immunosorbent assay (ELISA) for VEGFR-2 using human VEGF-R2/KDR ELISA kit [RBMS#2019R] according to manufacturer's instructions.

**2.2.5.2. Methodology.** The samples were diluted with assay buffer 1:25 determine the number of microwell strips required. Microwell strips were washed twice with wash buffer. 100  $\mu$ L assay buffer was added in duplicate and to all standard wells, 100  $\mu$ L of the prepared standard was pipetted into the first well and standard dilutions were created by transferring 100  $\mu$ L from well to well. 100  $\mu$ L of these standard dilutions were pipetted in the microwell strips, followed by addition of 100  $\mu$ L assay buffer in duplicate to the blank wells and 50  $\mu$ L assay buffer to sample wells. 50  $\mu$ L of the prediluted samples were added in duplicates to designated sample wells. 50  $\mu$ L of the prepared biotin-conjugate was added to all wells and then microwell strips were covered and incubated for 2 h at room temperature (18° to 25 °C). Microwell strips were washed six times with wash buffer and 100  $\mu$ L diluted Streptavidin-HRP was added to all wells. Microwell strips were covered again and incubated for 1 h at room temperature (18–25 °C). Microwell strips were washed six times with wash buffer and 100  $\mu$ L of TMB substrate solution was added to all wells. Incubation of the microwell strips for about 30 min at room temperature (18–25 °C) followed by addition of 100  $\mu$ L stop solution to all wells was done. Microwell reader was used to measure color intensity at 450 nm. The values of % activity versus a series of compound concentrations (0.01  $\mu$ M, 0.1  $\mu$ M, 1.0  $\mu$ M, 10  $\mu$ M, and 100  $\mu$ M) was then plotted using non-linear regression analysis of sigmoidal dose-response curve. The IC<sub>50</sub> values for compounds **5**



Reagents and conditions: a) i- EtONa/EtOH, rt, 2h; ii- PhNCS; 70 °C, 30 min. iii- ClCH<sub>2</sub>R, 60 °C, 30 min.; iv- EtONa, Reflux, 3h.

**Scheme 1.** Synthesis of thiophene derivatives **2a** and **2b**.

and **21** against VEGFR-2 was determined by the concentration causing a half-maximal percent activity and the data were compared with Sorafenib as standard VEGFR-2 inhibitor. Each experiment was repeated three times.

#### 2.2.6. Docking study

Molecular Operating Environment (MOE program 2008.10; Chemical Computing Group, Canada) was used to perform docking study. Crystal structures of VEGFR-2 complexed with sorafenib (PDB code 4ASD), and of tubulin (PDB ID: 1SA0) were downloaded from the protein data bank. The downloaded crystal structures were prepared for docking by adding the missing protons, deleting water molecules and all unnecessary co-crystallized ligands and metals using MOE software. Docking was performed using the default parameters of the software, and the best poses in terms of binding to the active site are discussed in text.

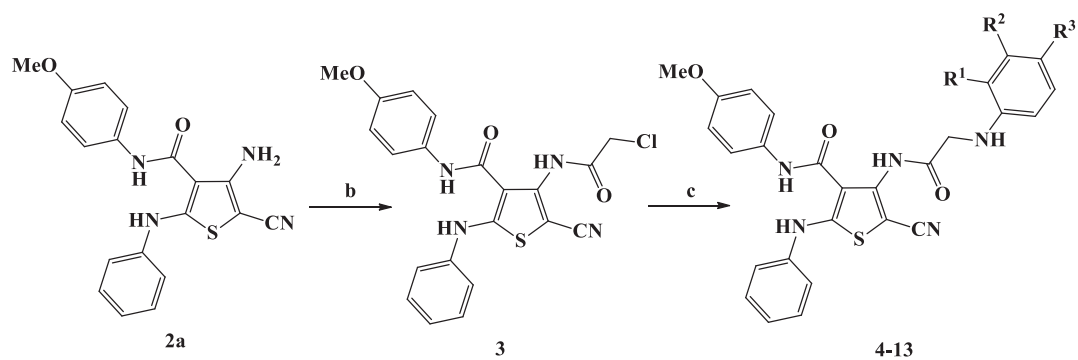
#### 2.2.7. QSAR study

The synthesized compounds were divided into two sets, the training set composed of 15 compounds **4–11**, **13–17**, **19–20** and **22–23** that was used for a QSAR model development and their IC<sub>50</sub> against HepG-2 cells were converted into the logarithmic scale (pIC) and an external test subset using the compounds **12**, **18** and **21** for validating the QSAR model was adopted. All the synthesized compounds were sketched in 2D and minimized by the protocol "Prepared Ligands" in the Discovery Studio 2.5 software (Accelrys Inc., San Diego, CA, USA). The values of cytotoxic activity (IC<sub>50</sub>) were converted into the logarithmic scale pIC<sub>50</sub> (pIC<sub>50</sub> = -log IC<sub>50</sub>) and then proceed to the QSAR analysis as the response variables. The obtained data set was further subdivided into the two subsets (Training and test set). Training set was composed of 15 compounds **4–11**, **13–17**, **19–20** and **22–23** and test set was three compounds **12**, **18** and **21**. The training set was used to build a regression model, and the test set was used to external evaluation of the predictive ability of the model obtained<sup>45</sup>. In this study, several molecular descriptors representing thermodynamic, electronic, spatial, structural, thermodynamic, geometric, topological and quantum mechanical properties were calculated using "Calculate Molecular Properties" protocol of the Discovery Studio 2.5 (Table S8), where all the descriptor values for the molecules were considered as independent variables while, the inhibitory concentration results (pIC<sub>50</sub>) were taken as dependent variables.

### 3. Results and discussion

#### 3.1. Chemistry

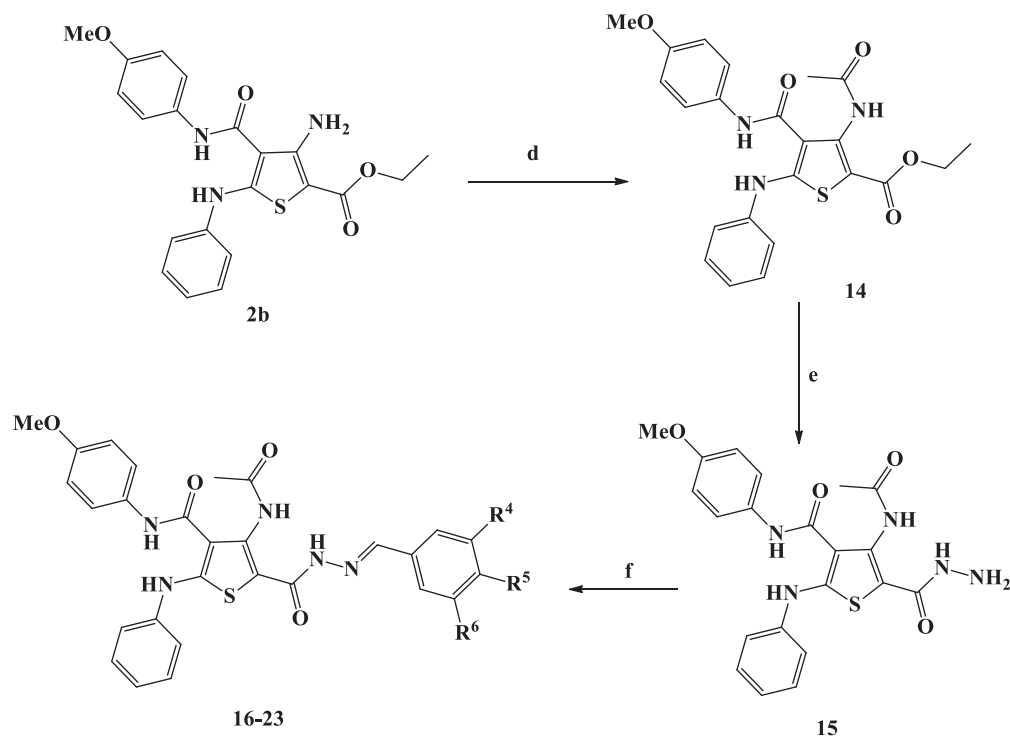
The work comprised the synthesis of two novel series of thiophene carboxamides; *N,N*-diaryl-2-amino-acetamido thiophenes **4–13** and arylidene thiophene hydrazides **16–23**. Two Microwave-assisted organic synthesis (MWAOS) methodologies are known, which are open vessel microwave-assisted organic synthesis (OVMAOS) and pressurized microwave-assisted organic synthesis (PMAOS). OVMAOS have the advantage of being safer than PMAOS, and could be used in a large scale which is suitable for industrial chemistry<sup>46,47</sup>. The final target compounds were synthesized under OVMAOS methodology. All synthetic procedures adopted for preparation of key intermediates **3**, **14**, **15** and final target thiophenes **4–13** and **16–23** are illustrated in Schemes 1–3. Adopting Gewald method<sup>48</sup>, phenyl isothiocyanate was reacted with alkaline solution of 2-cyano-*N*-(4-methoxyphenyl)acetamide **1**<sup>42</sup>, in absolute ethanol, followed by treatment with  $\alpha$ -halo active methylene compounds (chloro-acetonitrile or ethyl chloro-acetate) to yield thiophenes **2a** and **2b**, respectively (Scheme 1). <sup>1</sup>H NMR of thiophene derivatives **2a**, **b** showed two D<sub>2</sub>O exchangeable signals at  $\delta$  9.63–9.74 and 9.69–9.89 ppm corresponding to two NH protons, and another exchangeable signal of two protons at  $\delta$  10.18 for compound **2a** and  $\delta$  6.68 ppm for compound **2b**. Several synthetic trails for the preparation of compounds **2a** and **2b** were done under MWAOS but all experimental trails failed. Literature survey revealed that aryl carboxamides could be prepared by reaction of the corresponding aryl amines with acid halides in polar solvents as dioxane for 24 h at room temperature<sup>49</sup>. In this study, acylation of 4-aminothiophene derivative **2a** with chloro-acetyl chloride was performed in *n*-butanol as a high boiling solvent instead of ethanol and the reaction mixture was irradiated for 5 min at 150 °C to obtain the desired 4-(2-chloroacetamido)thiophene-3-carboxamide derivative **3** (Scheme 2). <sup>1</sup>H NMR spectrum revealed the disappearance of the amine NH<sub>2</sub> signal of the thiophene derivative **2a**, and the appearance of a singlet signal at  $\delta$  4.83 of two protons corresponding to chloromethylene protons. In addition, mass spectrum of compound **3** showed two molecular ion peaks at *m/z* 442 and 440 with 3:1 ratio (Cl pattern). Conventional nucleophilic substitution reaction of alkyl chloride as the 2-chloroacetamido derivatives with primary aromatic amines was reported in absolute ethanol and heating under reflux for long time (30 h)<sup>50</sup>. In the current investigation, a solution of the alkyl halide **3** in ethylene glycol was irradiated for 15 min with different aromatic amines and afforded 4-(2-*N*-arylamino-acetamido)thiophene-3-



**Reagents & conditions:** b)  $\text{ClCH}_2\text{COCl}$ , n-butanol, 150 °C, M.W, 5 min; c)  $\text{ArNH}_2$ , ethylene glycol, 120 °C, M.W, 15 min.

	R1	R2	R3		R1	R2	R3
4	H	H	H	9	H	H	$\text{OCH}_3$
5	H	H	Cl	10	H	H	$\text{NO}_2$
6	H	H	Br	11	Cl	H	H
7	H	H	$\text{CH}_3$	12	$\text{NO}_2$	H	H
8	H	H	OH	13	H	$\text{OCH}_3$	$\text{OCH}_3$

**Scheme 2.** Synthesis of 5-Cyano-N-(4-methoxyphenyl)-4-(2-arylaminoacetamido)thiophene-3-carboxamides 4–13.



	R4	R5	R6
16	H	H	H
17	H	Cl	H
18	H	Br	H
19	H	$\text{CH}_3$	H
20	H	$\text{OCH}_3$	H
21	H	$\text{OCH}_3$	OH
22	H	$\text{OCH}_3$	$\text{OCH}_3$
23	$\text{OCH}_3$	$\text{OCH}_3$	$\text{OCH}_3$

**Reagents & conditions:** d)  $\text{CH}_3\text{COCl}$ , n-butanol, 140 °C, M.W, 5 min; e)  $\text{NH}_2\text{NH}_2$ , n-butanol, 150 °C, M.W, 5 min; f)  $\text{ArCHO}$ , acetic acid, 100 °C, M.W, 15 min.

**Scheme 3.** Synthesis of 4-acetamido-5-(2-arylidenehydrazinocarbonyl)-N-(4-methoxyphenyl)-2-phenylaminothiophene-3-carboxamides 16–23.

carboxamides **4–13** (Scheme 2).  $^1\text{H}$  NMR spectra of the target compounds revealed the presence of two methylene protons and four exchangeable NH protons at  $\delta$  4.81–4.78 and  $\delta$  8.62–11.34 ppm, respectively. Moreover,  $^{13}\text{C}$  NMR spectra of thiophenes **4–13** displayed a cyano group at  $\delta$  111.0–112.9 ppm. To synthesize the target thiophene hydrazides **16–23**, amine group at C-3 of thiophene derivative **2b** must be protected. Masking of amine moiety via reaction with acyl halide as acetyl chloride is reported in dioxane as a reaction solvent<sup>49</sup>. In the present work, ethyl-3-amino-thiophene-2-carboxylate (**2b**) was treated with acetyl chloride to produce ethyl-3-acetamidothiophene-2-carboxylate derivative **14** (Scheme 3). The structure of intermediate **14** was confirmed by disappearance of the  $\text{NH}_2$  protons signal of the precursor **2b**, presence of signals corresponding to three NH protons at  $\delta$  9.56, 9.81, 10.08 ppm, and additional singlet signal of the acetyl protons at  $\delta$  2.26 in the  $^1\text{H}$  NMR spectrum of compound **14** (Scheme 3). The literature search disclosed that the ester group in ethyl thiophene-2-carboxylate derivatives could be converted into the corresponding acid hydrazides through hydrazinolysis of the parent ester in absolute ethanol and heating under reflux for 4 h<sup>51</sup>. Herein, hydrazinolysis of the ester group in the ethylthiophene-2-carboxylate **14** using hydrazine hydrate in *n*-butanol was performed by heating at 140 °C under OVMAOS conditions for 5 min which produced hydrazide **15** (Scheme 3). Modifying the carboxylic acid hydrazides to the corresponding arylidene derivatives could be achieved by heating equimolar amounts of the acid hydrazide with the appropriate aromatic aldehydes for 2 h either in absolute ethanol only or with acetic acid as a catalyst<sup>52</sup>. In the present work, the arylidene thiophene hydrazides **16–23** were synthesized *via* reacting 4-acetamido-5-hydrazinocarbonyl-*N*-(4-methoxyphenyl)-2-phenylamino thiophene-3-carboxamide (**15**) with different aromatic aldehydes in acetic acid as a reaction solvent and acid catalyst at 100 °C for 15 min under OVMAOS conditions (Scheme 3).  $^1\text{H}$  NMR spectra of *N*-arylidene thiophene hydrazides **16–23** showed the presence of azomethine protons ( $\text{N}=\text{CH}$ ) at  $\delta$  8.34–8.41 ppm, and confirmed the formation of the target small molecules.

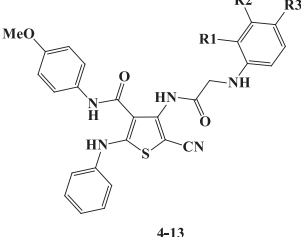
### 3.2. In vitro screening of the synthesized compounds 4–13 and 16–23

#### 3.2.1. In vitro cell growth inhibition of compounds 4–13 and 16–23 on HepG-2 and HCT-116 cancer cells

To assess cytotoxicity, liver hepatocellular carcinoma (HepG-2) and human colon carcinoma (HCT-116) cell lines were involved in this study, and Sulforhodamine-B stain (SRB) was used to assess cell viability according to the reported procedure<sup>43</sup>. Sorafenib was also tested as a control compound. Sorafenib showed  $\text{IC}_{50}$  values of 4.43 and 3.22  $\mu\text{M}$  against HepG-2 and HCT-116 cells, respectively.

**3.2.1.1. In vitro cytotoxic activity of *N,N'*-diaryl-2-amino-acetamide thiophenes 4–13 (model A) on HepG-2 and HCT-116 cells.** *N,N'*-Diaryl-2-aminoacetamide thiophene series (compounds **4–13**) displayed cytotoxic activity against both HepG-2 and HCT-116 cell lines with varying  $\text{IC}_{50}$  values. The most potent thiophene derivatives were compounds **5**, **6**, and **10**, which showed  $\text{IC}_{50}$  values of 1.92, 3.51, and 9.71  $\mu\text{M}$  on HepG-2 cells, and 7.83, 3.13, and 5.12  $\mu\text{M}$  on HCT-116 cells (Table 1 and Figure 4). All other analogs were less cytotoxic with  $\text{IC}_{50}$  values ranging from 10.42 to 74.32  $\mu\text{M}$  on HepG-2, and 10.28 to 64.11  $\mu\text{M}$  on HCT-116. Interestingly, compound **5** exhibited relatively higher cytotoxicity ( $\text{IC}_{50}$  value of 1.92  $\mu\text{M}$ ) than the reference compound sorafenib

**Table 1.**  $\text{IC}_{50}$  values of the 5-Cyano-*N*-(4-methoxyphenyl)-4-(2-*N*-(arylamino)acetamido)thiophene-3-carboxamide derivatives **4–13** against HepG-2 and HCT-116 cells.



Compound	$R^1$	$R^2$	$R^3$	$\text{IC}_{50}(\mu\text{M})^a$	
				HepG-2	HCT-116
<b>4</b>	H	H	H	74.32 $\pm$ 5.98	64.11 $\pm$ 7.51
<b>5</b>	H	H	4-Cl	1.92 $\pm$ 0.12	7.83 $\pm$ 0.61
<b>6</b>	H	H	4-Br	3.51 $\pm$ 0.22	3.13 $\pm$ 0.21
<b>7</b>	H	H	4-CH <sub>3</sub>	24.31 $\pm$ 1.96	18.41 $\pm$ 1.23
<b>8</b>	H	H	4-OH	10.42 $\pm$ 1.08	16.23 $\pm$ 1.52
<b>9</b>	H	H	4-OCH <sub>3</sub>	14.26 $\pm$ 1.23	21.35 $\pm$ 1.92
<b>10</b>	H	H	4-NO <sub>2</sub>	9.71 $\pm$ 0.86	5.12 $\pm$ 0.42
<b>11</b>	2-Cl	H	H	31.34 $\pm$ 3.61	52.21 $\pm$ 5.54
<b>12</b>	2-NO <sub>2</sub>	H	H	43.32 $\pm$ 4.23	60.11 $\pm$ 7.41
<b>13</b>	H	3-OCH <sub>3</sub>	4-OCH <sub>3</sub>	15.21 $\pm$ 1.62	10.28 $\pm$ 1.31

<sup>a</sup>The values given are means of three experiments.

( $\text{IC}_{50}$  value of 4.43  $\mu\text{M}$ ) with HepG-2 cells, while compound **6** exhibited the highest cytotoxicity ( $\text{IC}_{50}$  value of 3.13  $\mu\text{M}$ ) with HCT-116 cells (Table 1 and Figure 4).

**3.2.1.2. Structural activity relationship (SAR) of cytotoxic activity of *N,N'*-diaryl-2-amino-acetamide thiophenes 4–13.** Compounds **5** and **6** exhibited higher cytotoxicity than the rest of the compounds in the series, and compound **5** displayed cytotoxic effect with 2.31-fold higher than Sorafenib. Compound **6** was equipotent to Sorafenib. The results of the cytotoxicity screening experiments showed a correlation between the structural investigation of the compounds **4–13** with their cytotoxicity against HepG-2 and HCT-116 cells. Generally, substitution on the phenyl ring of the tail part contributed to cytotoxicity, while the unsubstituted derivative **4** was nearly not cytotoxic against HepG-2 and HCT-116 cells (Table 1 and Figure 5). The presence of an electron withdrawing group in the *para* position of the phenyl ring is essential for the observed cytotoxicity as in compounds **5**, **6**, and **10**. Importantly, the presence of an electron donating groups on the *para* position in compounds **7**, **8**, **9**, and **13** led to slight reduction of cytotoxicity compared to electron withdrawing groups containing compounds **5** and **6** (Table 1 and Figure 5). On the other hand, dramatic reduction in cytotoxicity was observed upon substituting the ring of the tail part on the *ortho* position as in (4-(2-(4-chlorophenylamino) acetamido)thiophene derivative **11** compared with (4-(2-(4-chlorophenylamino)acetamido) thiophene derivative **5** (Table 1 and Figure 5). It is worth mentioning that the most potent compounds **5** and **6** share a common pharmacophoric feature (a halogen in the *para* position) in the tail region with sorafenib, which might explain the high cytotoxicity observed in this experiment.

**3.2.1.3. In vitro cytotoxic activity of *N*-arylidene thiophene hydrazide derivatives 16–23 (model B) over HepG-2 and HCT-116 cells.** In this series, *N*-Arylidene thiophenehydrazides **20–23** showed good cytotoxicity against both cell lines with  $\text{IC}_{50}$  values in the range of 2.61–10.82  $\mu\text{M}$  with HepG-2 cell line, and 3.12–6.46  $\mu\text{M}$  with HCT-116 cell line (Table 2 and Figure 5).



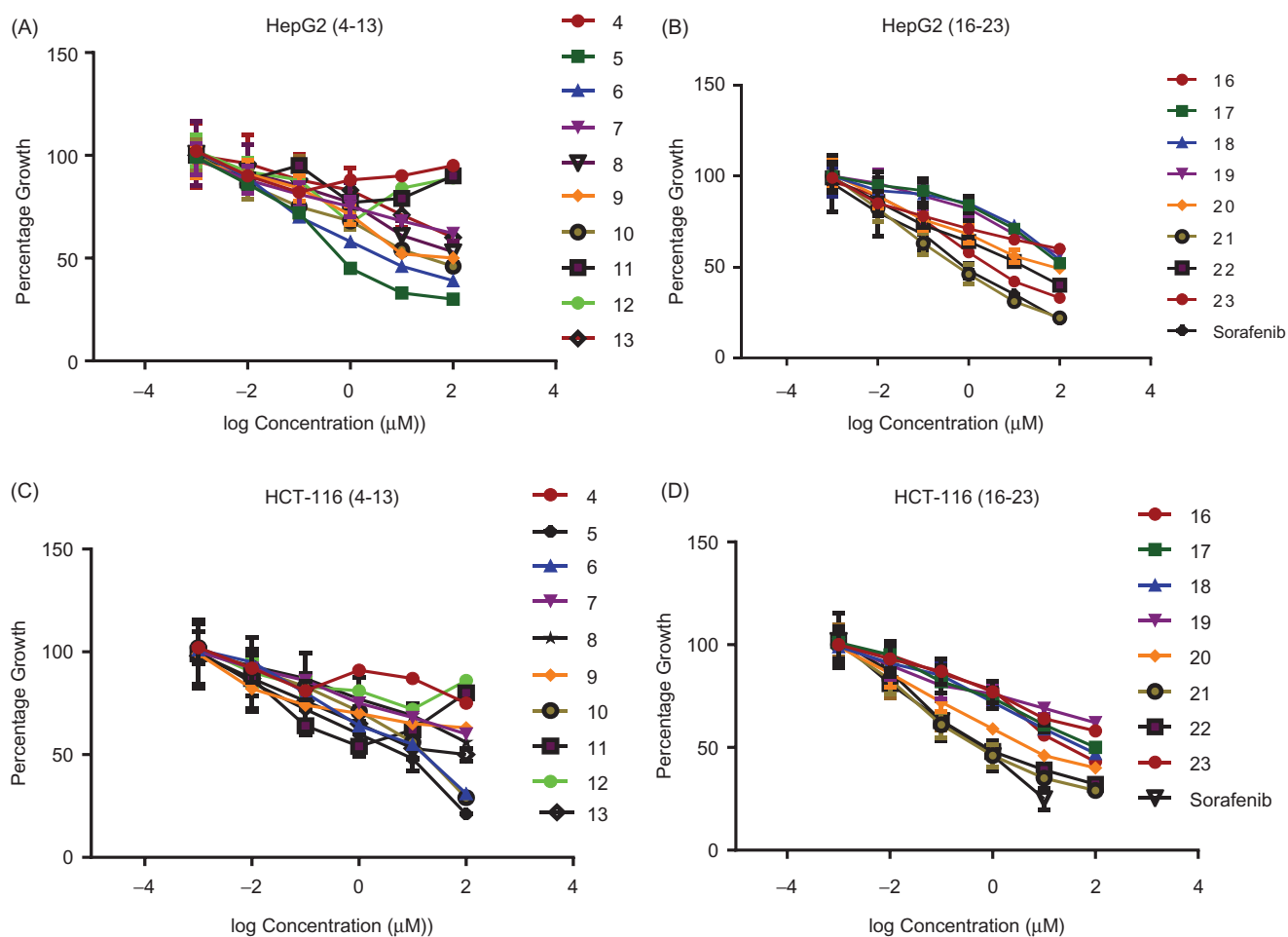


**Figure 4.** Dose response curves for the effect of the synthesized compounds 4–13 and 16–23 at different six concentrations (μM) on HepG-2 and HCT-116 cell lines for 24 h. (A) Effect of molecules 4–13 on Hep-G-2 cells. (B) Effect of molecules 16–23 on HepG-2 cells. (C) Effect of molecules 4–13 on HCT-116 cells. (D) Effect of molecules 16–23 on HCT-116 cells. Values represent the mean ± SEM for three experiments.

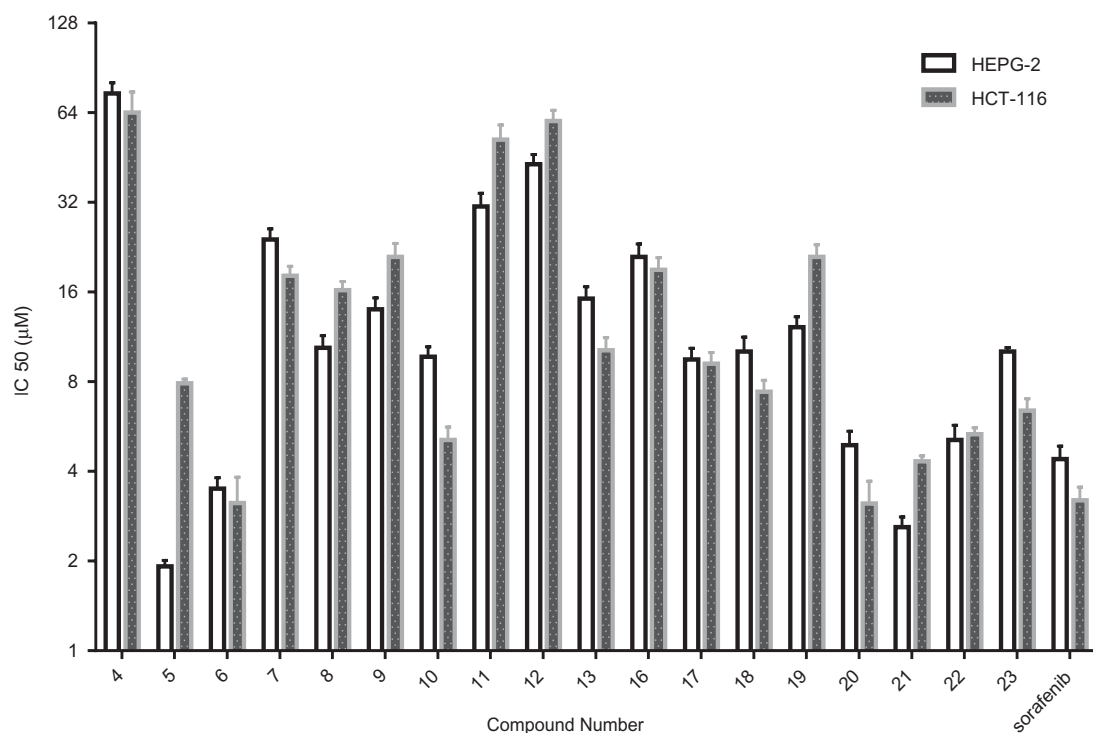
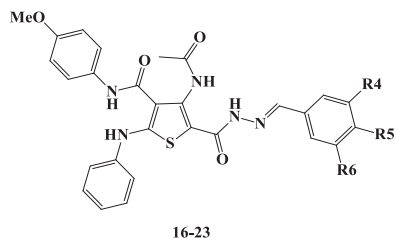


**Figure 5.** Graphical representation of IC<sub>50</sub> values (μM) of the synthesized compounds 4–13 and 16–23 against HepG-2 and HCT-116 cell lines.

**3.2.1.4. Structural activity relationship (SAR) of cytotoxic activity of *N*-arylidene thiophene hydrazides 16–23.** *N*-(3-Hydroxy-4-methoxybenzylidene) thiophene hydrazide **21** was the most potent cytotoxic agent (IC<sub>50</sub> value of 2.61  $\mu$ M) with about 1.7-fold

**Table 2.** IC<sub>50</sub> values of 4-acetamido-5-(2-arylidene-hydrazinocarbonyl)-*N*-(4-methoxyphenyl)thiophene-3-carboxamide derivatives **16–23** against HepG-2 and HCT-116 cells.



Compound	<i>R</i> <sup>4</sup>	<i>R</i> <sup>5</sup>	<i>R</i> <sup>6</sup>	IC <sub>50</sub> ( $\mu$ M) <sup>a</sup>	
				HepG-2	HCT-116
<b>16</b>	–H	–H	–H	21.41 $\pm$ 2.91	19.21 $\pm$ 1.46
<b>17</b>	–H	–Cl	–H	9.50 $\pm$ 0.86	9.24 $\pm$ 1.02
<b>18</b>	–H	–Br	–H	10.13 $\pm$ 1.12	7.41 $\pm$ 0.62
<b>19</b>	–H	CH <sub>3</sub>	–H	12.21 $\pm$ 1.31	21.45 $\pm$ 1.82
<b>20</b>	–H	–OCH <sub>3</sub>	–H	4.96 $\pm$ 0.45	3.12 $\pm$ 0.31
<b>21</b>	–H	–OCH <sub>3</sub>	–OH	2.61 $\pm$ 0.12	4.32 $\pm$ 0.11
<b>22</b>	–H	–OCH <sub>3</sub>	–OCH <sub>3</sub>	5.12 $\pm$ 0.45	5.33 $\pm$ 0.37
<b>23</b>	–OCH <sub>3</sub>	–OCH <sub>3</sub>	–OCH <sub>3</sub>	10.82 $\pm$ 0.065	6.46 $\pm$ 0.49

<sup>a</sup>The values given are means of three experiments.

higher cytotoxicity compared to Sorafenib (IC<sub>50</sub> value of 4.43  $\mu$ M). *N*-(4-methoxybenzylidene) thiophene hydrazide **20** was the most active (IC<sub>50</sub> value of 3.12  $\mu$ M) and almost equipotent to the reference compound. Remarkably, compound **21** possessed more cytotoxic effect within the series on HepG-2, while compound **20** exhibited the most potent cytotoxicity on HCT-116 cells (Table 2 and Figure 5). Within the *N*-arylidene thiophene hydrazide series **16–23**, investigation of the electronic nature of the arylidene moieties in the tail part showed that hydrazides **20** and **21** that contain one methoxy group on arylidene groups exhibited higher cytotoxicity than compounds **17–18** which contain a halogen on the same position. The increased cytotoxicity might be due to the structural similarities of arylidene moieties of compounds **20–23** with the potent anti-mitotic compounds as colchicine and CA-4 (Figures 2 and 3). Analysis of the structural variations between the *N,N'*-diaryl-2-aminoacetamide thiophenes (model A) and arylidene thiophene hydrazide (model B) demonstrated that the presence of electron withdrawing substituents on the aryl rings of the tail part in *N,N'*-diaryl-2-aminoacetamide thiophenes (**5, 6**, and **10**) is essential for cytotoxic activity. On the other hand, an arylidene group bearing electron donating group in the tail part of model B (compounds **20–23**) seems to be also crucial for the observed good cytotoxicity. Collectively, this experiment revealed the presence of a significant correlation between the linker (spacer) moiety and the substitution pattern on the aryl ring in the tail part. Furthermore, the electronic properties of the substituents on the aryl ring exert an additional effect on cytotoxic activity. Finally, the cytotoxicity results for the synthesized

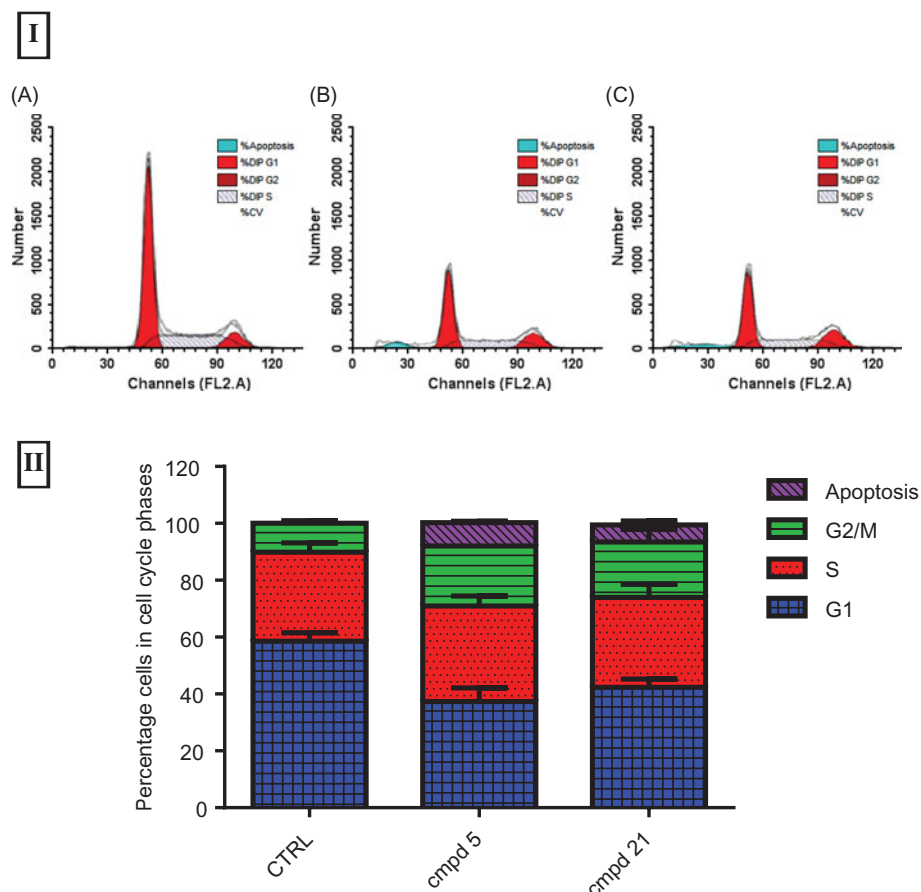


**Figure 6.** (I) Flow cytometric analysis of the most potent compounds **5** and **21** on cell cycle distribution of HepG-2 cancer cells (24 h). (A) Control HepG-2 cells. (B) Cells treated with compound **5** (2.61  $\mu$ M) 24 h showing most of the cells arrested in G2/M phase and apoptosis. (C) Cells treated with compound **21** (1.92  $\mu$ M) for 24 h showing cell cycle arrest at G2/M phase. (II) Data expressed as mean ( $n = 4$  experiments)  $\pm$  SEM and statistical comparisons were carried out using one-way analysis of variance (ANOVA) followed by Tukey multiple comparisons.

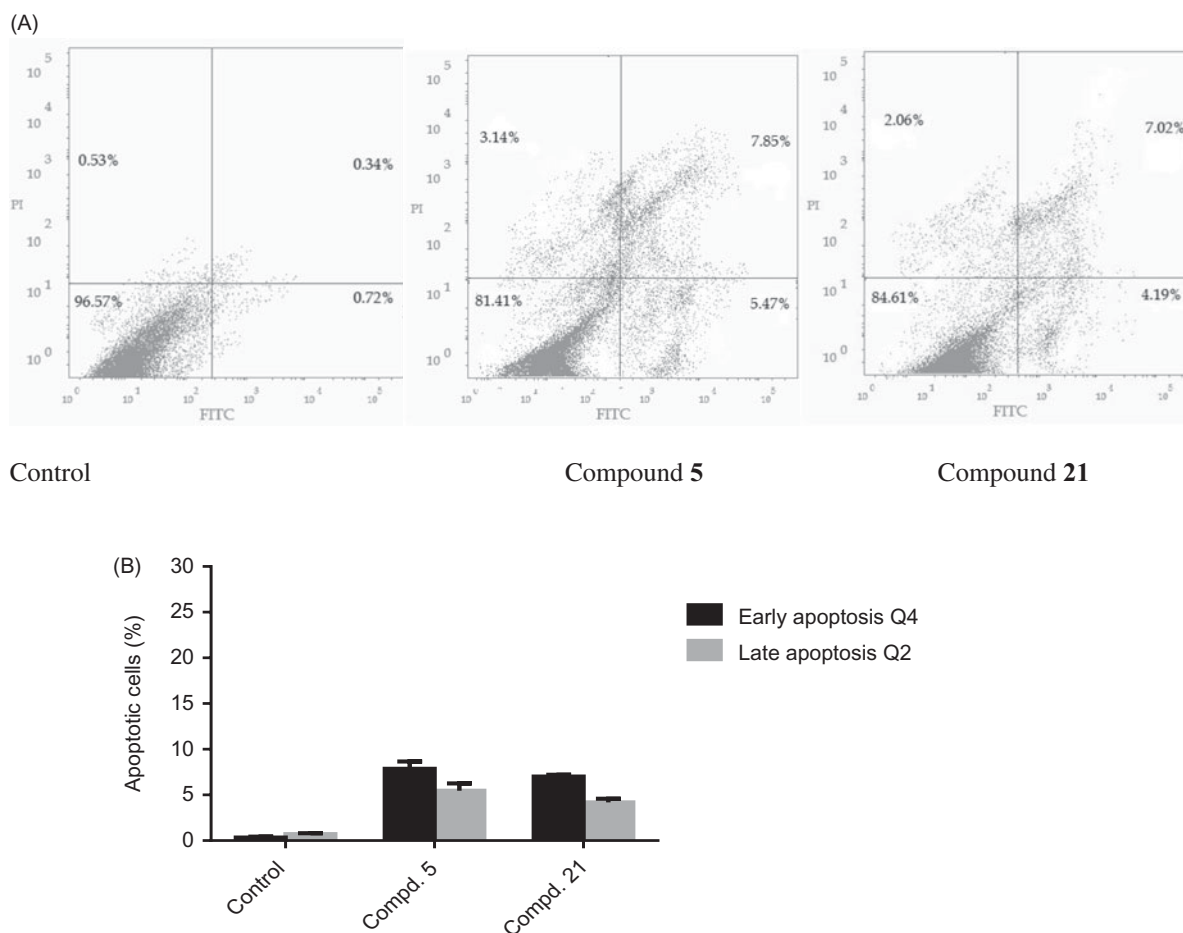


**Figure 7.** FITC-annexin-V and PI staining of HepG-2 cells after treatment with compounds **5** and **21** at their  $IC_{50}$  values. (A) Dot plots showing: dead cells and cells debris (Q1, top left quadrant), late apoptosis cells (Q2, top right quadrant), viable cells (Q3, bottom left quadrant), and early apoptosis cells (Q4, bottom right quadrant). (B) Graphical representation of the early and late apoptotic cells percentage upon treatment with **5**, **21** or no treatment control.

compounds showed higher cytotoxic sensitivity over HepG-2 cancer cells than HCT-116 cells.

### 3.2.2. In vitro DNA-flow cytometry and detection of apoptosis for compounds **5** and **21** on HepG-2 cells

The most cytotoxic thiophene derivatives **5** and **21** were selected to further evaluate their effect on the cell cycle progression and induction of apoptosis. HepG-2 cells were treated with each derivative at its  $IC_{50}$  values for 24 h, and then the DNA content was analyzed by flow cytometry using FACS Calibur (Becton Dickinson). A control experiment with no treatment was also included. Flow cytometric analysis revealed that treatment with compound **5** and **21** resulted in apoptosis as denoted by the increase in the apoptotic sub-G1 cell population (8.23% and 6.07%, respectively), compared with the control (0.10%) (Figure 6 and Table S3). In addition, a G2/M arrest was also observed upon treatment with compounds **5** or **21**, with about 2- and 1.9-fold increase compared to the control (Figure 6 and Table S3). Accumulation of cells in the G0 phase and cell cycle arrest at G2/M phase indicates the possible role of compounds **5** and **21** in apoptosis induction and cell death. In conclusion, compounds **5** and **21** showed pre-apoptotic activity and cell growth inhibition through cell cycle arrest at G2/M phase. *N*-aryl-2-*N*-(4-chlorophenyl) amino-acetamide **5** showed higher apoptotic inducing activity than *N*-(3-hydroxy-4-methoxybenzylidene) thiophene hydrazide **21**.

### 3.2.3. In vitro apoptosis identification by FITC-annexin V-staining

To further assess the tumour suppression property of the compounds, and to confirm that the observed sub-G1 cells accumulation was due to apoptosis, HepG-2 cells treated with **5** and **21** for 24 h were analyzed with PI and FITC-annexin V stain for apoptosis determination (Figure 7 and Table S4). Both early apoptosis (Q4 quadrant in Figure 7(A)) and late apoptosis (Q2 quadrant in Figure 7(A)) stages in HepG-2 cells increased after treatment with compounds **5** and **21** (Figure 7). Interestingly, the late apoptotic cells percentage showed an increase after treatment with compounds **5** and **21** from 0.34% in control to 7.85% (23-fold increase) and 7.2% (21-fold increase). In addition, early apoptosis was significantly increased from 0.72% in the no treatment control to 5.47% (8-fold increase) and 4.29% (6-fold increase) upon treatment with **5** and **21**, respectively. Furthermore, a profile of early apoptotic cell population was also observed for the tested compounds **5** and **21**. The results in this experiment are in line with the previous experiment, and confirm that these compounds exhibit their cytotoxic effect and pro-apoptotic activity.

### 3.2.4. In vitro measurement of the concentration of the apoptotic marker proteins (*p53*, *bax*, *bcl-2*, *caspase-3/7*) for compounds **5** and **21** in HepG-2 cells

To further investigate the apoptosis inducing activity of *N,N'*-diaryl-2-amino-acetamide **5** and *N*-arylidene hydrazide **21**, the levels

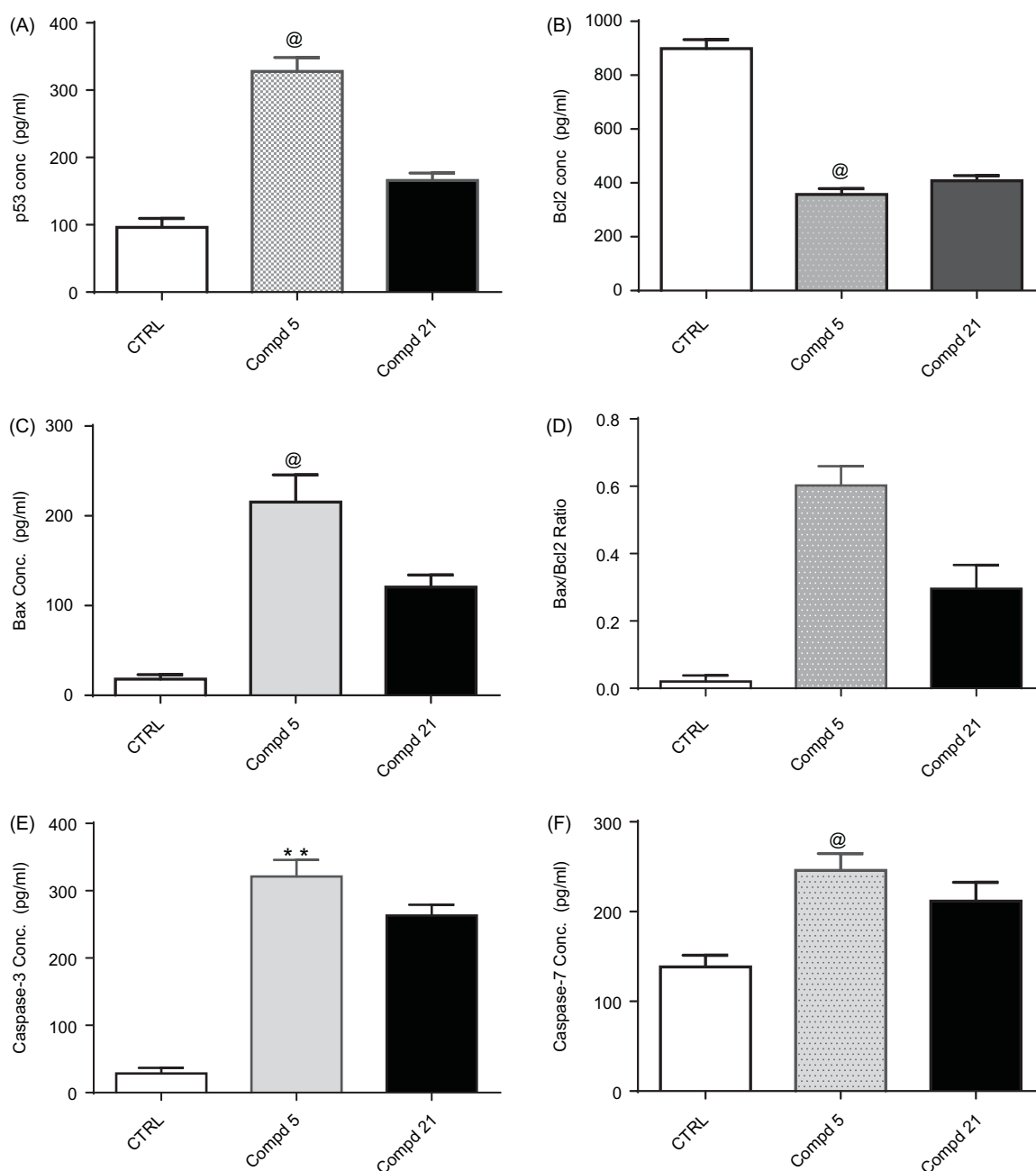


**Figure 8.** *In vitro* ELISA immunoassay measurement of the p53, Bcl-2, Bax, caspase-3 and caspase-7 concentration in HepG-2 cells after treatment for 24 h with thiophene-3-carboxamides **5** and **21** at their  $IC_{50}$ . (A) effect of compounds **5** and **21** on p53 concentration (B) effect of compounds **5** and **21** on Bcl-2 concentration (C) effect of compounds **5** and **21** on Bax concentration (D) effect of compound **5** and **21** on Bax/Bcl-2 ratio (E) effect of compounds **5** and **21** on caspase-3 concentration (F) effect of compounds **5** and **21** on caspase-7 concentration. Data were expressed as mean ( $n = 3$  experiments)  $\pm$  SEM and statistical comparisons were carried out using one-way analysis of variance (ANOVA) followed by Tukey multiple comparisons test at  $p < .05$ .

**Table 3.**  $IC_{50}$  values ( $\mu M$ ) of thiophene-3-carboxamides **5**, **6**, **10**, **17**, **20–23**, sorafenib, and colchicine in VEGFR-2 enzyme assay, and  $\beta$ -tubulin polymerization inhibition, along with the  $IC_{50}$  values with HepG-2 cell line.

Compound	VEGFR-2 <sup>a</sup>	% $\beta$ -TUB polymerization inhibition	HepG-2
<b>5</b>	$0.59 \pm 0.21$	$72.61 \pm 0.14$	1.92
<b>6</b>	$0.93 \pm 0.19$	ND	3.51
<b>10</b>	$3.92 \pm 0.16$	ND	9.71
<b>17</b>	$5.91 \pm 0.23$	ND	9.50
<b>20</b>	$1.71 \pm 0.21$	ND	4.96
<b>21</b>	$1.29 \pm 0.13$	$85.95 \pm 0.21$	2.61
<b>22</b>	$1.80 \pm 0.17$	ND	5.10
<b>23</b>	$5.21 \pm 0.32$	ND	10.78
Sorafenib	$2.07 \pm 0.15$	ND	4.43
Colchicine	ND	$90.62 \pm 0.24$	ND

<sup>a</sup>The values given are means of three experiments. ND, not determined.

of apoptosis-induction biomarkers, p53, Bax, Bcl-2, caspase-3/7 proteins were measured after 24 h treatment of HepG-2 cells with compound **5** or compound **21** at their  $IC_{50}$  values, and were then compared with a no treatment control (Figure 8 and Table S5). The tumour suppression gene, p53, is a transcription factor that blocks cell cycle at G1 phase and induces apoptosis *via* mitochondrial pathway through several proteins such as Bax and Bcl-2 via loss of cell contents and restriction of cell growth. In this experiment, treatment of HepG-2 cells with compounds **5** and **21** led to significant increase in p53 protein level, with about 3.4- and 1.7-fold increase, respectively, compared with the control (Figure 8(A) and Table S5). This result suggests that compounds **5** and **21** caused an elevation



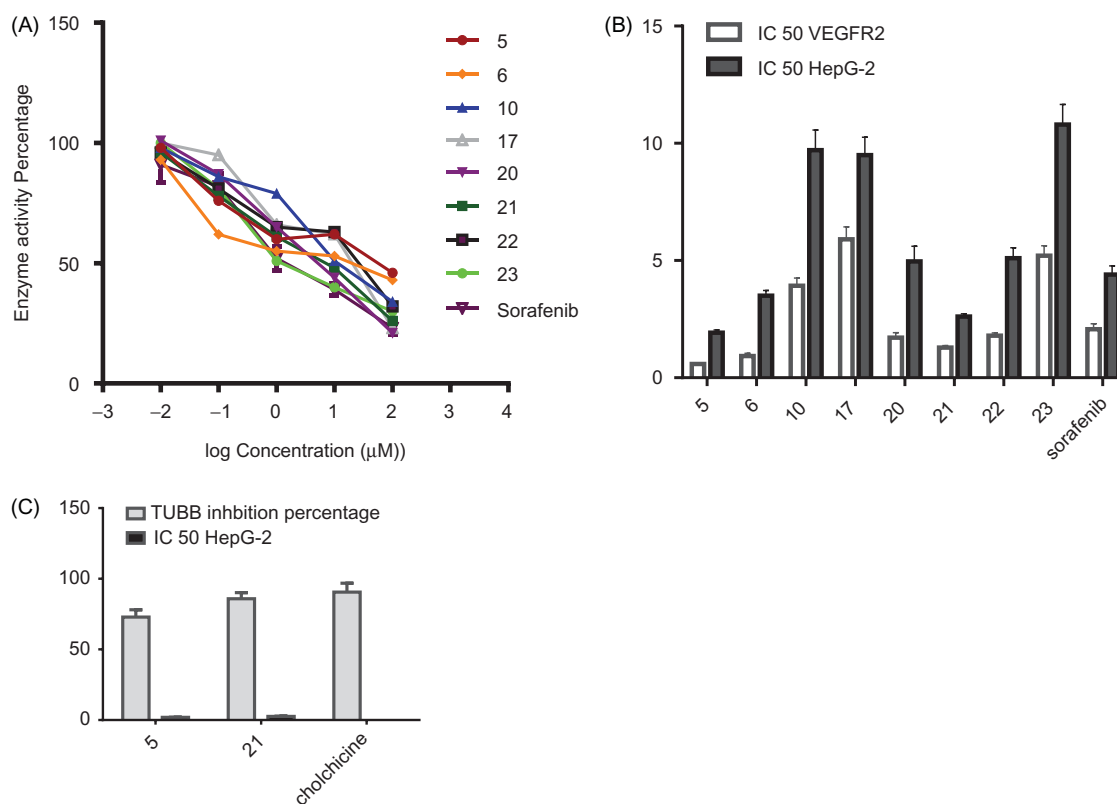


**Figure 9.** (A) Dose response curve for compounds **5**, **6**, **10**, **17**, **20–23** and Sorafenib for IC<sub>50</sub> determination of VEGFR-2 enzyme. Values represent the mean  $\pm$  SE for four experiments. (B) Graphical representation of IC<sub>50</sub> for compounds **5**, **6**, **10**, **17**, **20–23** and Sorafenib on VEGFR-2 enzyme, HepG-2 cells. (C) Graphical representation of IC<sub>50</sub> for compounds **5**, **21** on HepG-2 cells and  $\beta$ -tubulin inhibition percentage of compounds **5** and **21** compared with colchicine. Values represent the mean  $\pm$  SE for two experiments.

in the concentration of p53, which might have led to the observed cell growth inhibition and apoptosis induction. Among the resistance mechanisms of tumour cells to apoptosis is the increase in the expression of anti-apoptotic proteins, such as Bcl-2, and the decrease of the expression of pro-apoptotic proteins, such as Bax<sup>53</sup>. Treatment of HepG-2 cells with compounds **5** and **21** resulted in a significant increase in the level of Bax by 6.6- and 11.8-fold, respectively compared to the control (Figure 8(C) and Table S4). On the other hand, levels of Bcl-2 decreased by 2.2- and 2.5-fold, respectively compared to the control (Figure 8(B) and Table S5). Finally, the tested compounds **5** and **21** showed significant higher Bax/Bcl-2 ratio than the control, which is consistent with the results of the DNA-flow cytometry that revealed the ability of compounds **5** and **21** to induce apoptosis in HepG-2 cells (Figure 8(D)).

Activation of caspase-3/7 is the final effective step in apoptosis induction leading to DNA fragmentation and cell death<sup>54</sup>. Moreover, it was suggested that the caspase proteins family –especially caspase-7– are potentially involved in the regulation at M phase<sup>55</sup>. Given that compounds **5** and **21** significantly elevated Bax/Bcl-2 ratio, we were encouraged to subsequently evaluate the effect of these derivatives on the levels of active caspase-3/7 upon treatment of HepG-2 cells. As expected, compound **5** increased the level of caspase-3/7 by about 11.2- and 6.9-fold, respectively compared to the control, while compound **21** increased the level of caspase-3/7 by 9.2- and 5.9-fold, respectively compared to the control (Figures 8(E, F)). In conclusion, compound **5** showed a pro-apoptotic effect higher than compound **21**, through increasing p53 protein level, Bax/Bcl-2 ratio, and levels of the terminal caspase-3/7, which supported the results obtained from cell cycle analysis (Figure 8).

### 3.2.5. In vitro screening against vascular endothelial growth factor receptor-2 (VEGFR-2) enzyme for *N,N'*-diaryl-2-amino-acetamides **5**, **6**, **10** and *N*-arylidene thiophene hydrazides **17** and **20–23**

To assess the success of the approach used to design the pharmacophores developed in this work as VEGFR inhibitor, we extended the biological investigation to determine VEGFR-2 enzyme inhibitory activity of the analogs. The IC<sub>50</sub> values of the most promising cytotoxic derivatives in each library (*N,N'*-diaryl-2-amino-acetamides **5**, **6**, and **10** from model A, and *N*-arylidene thiophene hydrazides **17**, **20–23** from model B) were determined. Sorafenib, as a reference VEGFR-2 inhibitor was also tested as positive control (Table 3 and Figures 9(A,B)). The *N,N'*-diaryl-amino-acetamide derivatives **5**, **6**, and **10** showed IC<sub>50</sub> values in the range of 0.59–3.92  $\mu\text{M}$ , which is nearly equipotent to standard drug Sorafenib (IC<sub>50</sub> value of 2.07  $\mu\text{M}$ ). Significantly, compounds **5** and **6** showed IC<sub>50</sub> value of 0.59 and 0.93  $\mu\text{M}$ , which are potent than Sorafenib. The results point to the likelihood that the good inhibitory activity displayed by the 5-cyano-*N*-(4-methoxyphenyl)-4-(2-(arylamino) acetamido) thiophene-3-carboxamide derivatives **5**, **6**, and **10** might be due to the structural similarity in molecular skeleton to the second generation *ortho*-uriedo-aryl carboxamide VEGFR-2 inhibitors, such as XL-880 and CP-547-623, in addition to structural similarities with tail part of Sorafenib (Table 3 and Figures 9(A,B)). In parallel, *N*-arylidene thiophene hydrazides **17** and **20–23** that belong to pharmacophoric model B showed good inhibitory activities, with the lowest activity observed in *N*-(4-chlorobenzylidene)thiophene hydrazide **17** and *N*-(3,4,5-trimethoxybenzylidene)thiophene hydrazide **23**. It's worth mentioning that

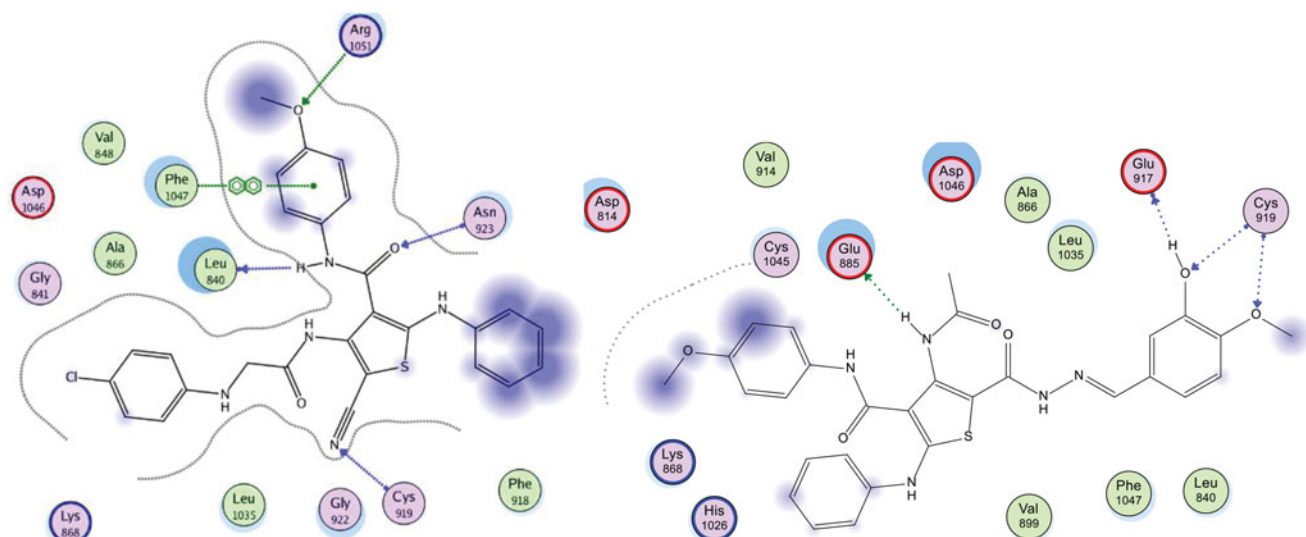


Figure 10. Docking poses displaying 2D interactions of compounds **5** (left) and **21** (right) with VEGFR-2 active site.

compound **23** bears a bulky tri-methoxyphenyl moiety, which could explain its lower inhibitory activity among the series. The most potent analog in compounds **16–23** was compound **21**, which displayed a slightly lower  $IC_{50}$  value ( $1.29 \mu M$ ) than the reference compound Sorafenib ( $IC_{50}$  value of  $2.07 \mu M$ ) (Table 3).

### 3.2.6. In vitro $\beta$ -tubulin polymerization inhibition assay (TUB) for *N,N'*-diaryl-2-aminoacetamide **5** and *N*-arylidene hydrazide **21** on HepG-2 cells

To investigate the growth inhibition showed by the synthesized compounds **5** and **21** and the observed cell cycle arrest at G2/M phase, further enzyme assay for  $\beta$ -tubulin polymerization inhibition percentage on HepG-2 was carried out at their  $IC_{50}$  values. The inhibitory activity in this experiment is given as the percentage of  $\beta$ -tubulin polymerization inhibition. The obtained results showed that compounds **5** and **21** produced promising tubulin polymerization suppression compared with colchicine (Table 3 and Figure 9(C)). Compounds **5** and **21** showed 73% and 86%  $\beta$ -tubulin polymerization inhibition, respectively. Compound **21** was nearly equipotent to colchicine, while compound **5** exhibited lower inhibition percentage, compared with the reference anti-mitotic drug, Colchicine (Table 3). The observed inhibitory activity of compound **21** might be due to close structural similarities to CSI inhibitors (Table 3). On the other hand, the obtained tubulin polymerization inhibition for *N*-aryl-2-*N*-(4-chlorophenyl) aminoacetamide **5** suggested that it is one of atypical CSI agents. In summary, the good inhibitory activity against  $\beta$ -tubulin polymerization for compounds **5** and **21** might explain the cell cycle block at G2/M phase exhibited by **5** and **21** in the previous experiments and supports the hypothesized design of the pharmacophoric models mentioned in this work.

## 3.3. Molecular docking studies

### 3.3.1. Molecular docking in the active site of VEGFR-2 enzyme

Docking study was done to assess the binding affinities of the most active thiophenes **5** and **21** in VEGFR-2 active site. The crystal structure of VEGFR-2 (PDB ID:4ASD) enzyme co-crystallized with sorafenib was used in this study. Compounds **5** and **21** showed promising binding affinity with VEGFR-2, as both inhibitors occupied the active site of the enzyme. The co-crystallized

ligand, sorafenib formed four H-bonding interactions with Glu885, Cys919, and Asp1046 amino acid residues in the VEGFR-2 active site (Figure S58). Compound **5** formed four hydrogen bonding interaction with Leu840, Cys919, Asn923, and Arg1051, in addition to arene-arene interaction with Phe1047, total 5 binding interactions with the active site of VEGFR-2 (Figure 10). On the other hand, **21** showed four hydrogen bonding interactions with Glu885, Glu917, and Cys919 (Figure 10). This study shows that the binding interactions of derivatives **5** and **21** to the active site of VEGFR-2 are similar to Sorafenib, which explains the low  $IC_{50}$  values observed with VEGFR-2 in this work (Table 3).

### 3.3.2. Molecular docking in tubulin colchicine binding site

To evaluate the binding of analogs **5** and **21** to colchicine binding site of tubulin, a docking study was carried out with the colchicine binding site in the x-ray crystal structure of tubulin (PDB ID: 1SA0). Both compounds **5** and **21** occupied colchicine binding site of the enzyme. Compounds **5** showed good binding interactions with two hydrogen bonds with ThrA179 and LysB254 (Figure 11). In addition, **21** bound to the active site with two hydrogen bonds with SerA178 and TyrB202 (Figure 11). Aromatic rings in both derivatives displayed favorable hydrophobic interactions with different amino acids lining the active site and the active site entrance (Leu245, Lys251, Lys 341, Leu 242, Val 307, Ile 359 and Leu 252). The results of this docking study are in agreement with the  $\beta$ -tubulin polymerization inhibition assay (Table 3), where both studies suggest that compounds **5** and **21** bind to the colchicine binding site of  $\beta$ -tubulin, and can act as  $\beta$ -tubulin polymerization inhibitors (Table 3 and Figure 11).

## 3.4. Quantitative structure activity relationship (QSAR)

To validate the results of cytotoxicity against HepG-2 cancer cells, QASR model was generated. The synthesized compounds were divided into 2 sets, the training set is composed of 15 compounds (**4–11**, **13–17**, **19–20** and **22–23**). The training set was used to develop the QSAR model in which their  $IC_{50}$  against HepG-2 cells were converted into the logarithmic scale (pIC), while compounds **12**, **18** and **21** were used in the external test subset to validate the developed QSAR model.

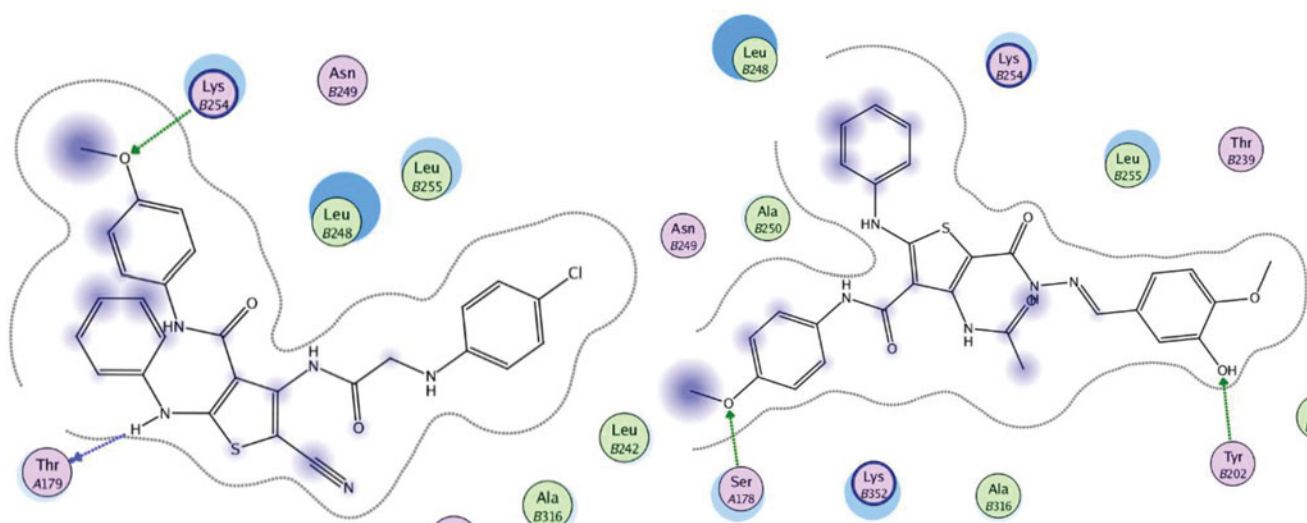


Figure 11. Docking poses displaying 2D interactions of compounds 5 (left) and 21 (right) with tubulin colchicine binding site.

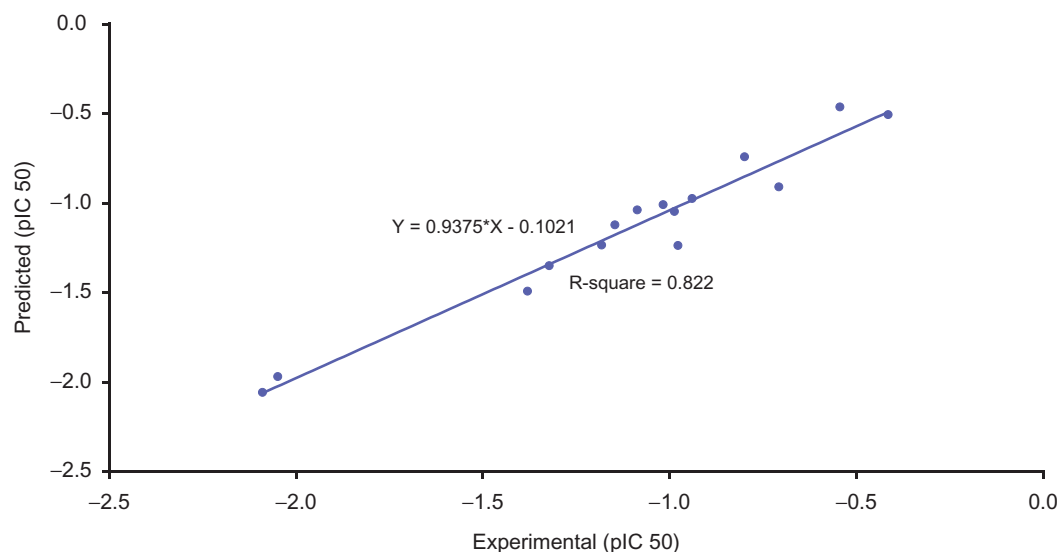


Figure 12. Plot of predicted versus experimental  $pIC_{50}$  values of the training set compounds and results against HepG-2 human tumor cell line according to QSAR equation.

### 3.4.1. Development of QSAR model

Several molecular descriptors were calculated for each compound employing a calculated molecular properties module. The 3D structures of the training set compounds were imported into the Discovery Studio program to calculate various molecular descriptors including energies of highest occupied and lowest unoccupied molecular orbitals (HOMO and LUMO) for each of the synthesized compound<sup>39</sup>. First, Genetic function approximation (GFA) which is a useful statistical analysis tool to correlate biological activity or property with chemical characteristics of molecules was employed to search for the best possible QSAR regression equation, then Multiple linear regression (MLR) analysis were employed to optimize QSAR model<sup>39</sup>. The MLRTemp Model equation bearing the relevant descriptors shows our best performing QSAR models is given as the following equation:

$$pIC_{50} = 25786 - 721 \times \text{Jurs} - \text{RPCS} - 14675 \times \text{RadofGyration} + 199.27 \times \text{PMI} - \text{Mag} + 143.49 \times \text{PMI} - \text{X} - 287.36 \times \text{PMI} - \text{Z}$$

According to the equation, the QSAR model was represented graphically by scattering plots of the experimental cytotoxic

Table 4. Estimated  $pIC_{50}$  data of the training set analogs against HepG-2 cell line according to QSAR Equation.

Compound	Experimental cytotoxicity $pIC_{50}$	Predicted cytotoxicity $pIC_{50}$	Residual
4	-2.08990	-2.05690	-0.03300
5	-0.41497	-0.50514	0.09017
6	-0.54406	-0.46239	-0.08167
7	-1.38021	-1.49136	0.11115
8	-1.01703	-1.00827	-0.00876
9	-1.14612	-1.12057	-0.02555
10	-0.98677	-1.04532	0.05855
11	-2.04921	-1.96848	-0.08073
13	-1.18184	-1.23299	0.05115
16	-1.32221	-1.34830	0.02609
17	-0.97772	-1.23552	0.25780
19	-1.08635	-1.03742	-0.04893
20	-0.93951	-0.97312	0.03361
22	-0.79934	-0.74036	-0.05898
23	-0.70757	-0.90848	0.20091

activity  $pIC_{50}$  versus the predicted activity values  $pIC_{50}$  for the training set compounds against HepG-2 cells as (Figure 12).

**Table 5.** External validation for the established QSAR model utilizing potent (21), moderate (18) and inactive (12) anticancer active agents.

Compound	Experimental cytotoxicity pIC <sub>50</sub>	Predicted cytotoxicity pIC <sub>50</sub>	Residual
12	−2.15533	−2.18184	0.02651
18	−1.01703	−1.16136	0.14433
21	−0.27875	≤0.36172	0.08297

### 3.4.2. Validation of QSAR model

QSAR model was validated employing leave one-out cross-validation by setting the folds to a number much larger than the number of samples,  $r^2$  (squared correlation coefficient value) and  $r^2_{\text{prediction}}$  (predictive squared correlation coefficient value), residuals between the predicted and experimental activity of the training set (Table 4), ( $N = 15$ ,  $r^2 = 0.822$ ,  $r^2_{\text{adj}} = 0.745$ ,  $r^2_{\text{pred}} = 0.708$ ), where  $N$ , represents number of compounds in the training set,  $r^2$  (adj) is  $r^2$  adjusted for the number of terms in the model,  $r^2$  (pred) is the prediction  $r^2$ , equivalent to  $q^2$  from a leave one-out cross-validation.

### 3.4.3. External validation of QSAR

In addition to validation of QSAR model by employing leave one-out cross-validation,  $r^2_{\text{adj}}$  and  $r^2_{\text{pred}}$ , external validation of the determined QSAR equations was performed utilizing three of compounds exhibiting potent (21), moderate (18) and inactive (12) anticancer properties. The observed pIC<sub>50</sub> activities and those provided by QSAR study and residuals between the predicted and experimental activity of the test set are shown in Table 5. It should be noted that the predicted cytotoxic activity by QSAR model was very close to the experimentally observed values. In conclusion, descriptors which played important role in developing QSAR model were jurs-RPCS. Jurs-RPCS indicated that the relative hydrophobic characters of the whole molecule are important for the observed activity. Other descriptors used were Radius of gyration (Rad of Gyration), which is a geometrical descriptor and measure of the size of the molecule. Another important descriptor was the principal moment of inertia (PMI), which is a physical property that is related to the rotational dynamics of a molecule that combine shape and electronic information to characterize molecules<sup>56</sup>. QSAR model suggested that the cytotoxic activity of the two models A and B was affected by electronic effect of the substituents and shape of the molecule as previously explained in the cytotoxicity results.

## 4. Conclusions

In this study, a library of small synthetic molecules sharing a common *ortho*-aminothiophene carboxamide moiety was designed as dual anti-angiogenesis agents and antimitotic agents. The therapeutic rationale behind the design of compounds with dual biological targets was to decrease the acquired resistance of tumour cells towards hypoxia induced by these molecules and hence improved apoptosis induction by the anti-angiogenic drugs. The *ortho*-aminothiophene carboxamides 4–13 and 16–23 were synthesized under microwave assisted synthesis protocol in good yield as prerequisite for sustainable development of organic synthesis. The *N,N'*-diaryl-2-amino-acetamide thiophenes 4–13 and *N*-arylidene thiophene hydrazides 16–23 were evaluated for their *in vitro* anti-proliferative activity against gastrointestinal solid cancer cell lines (HepG-2 and HCT-116). The most cytotoxic compounds with both cancer cells were 5 and 21. Compound 5 showed higher cytotoxic activity on HepG-2 cells than Sorafenib with 2.3-fold, while the restricted conformation hydrazide derivative 21

displayed 1.7-fold higher cytotoxicity compared to Sorafenib. Moreover, compounds 5 and 21 showed pro-apoptotic activity by inducing significant increase in the percentage of apoptotic cells (8.23% and 6.07%, respectively) in DNA-flow cytometry compared to control (0.10%), indicating potent apoptosis-inducing cancer cell death. The apoptosis mechanistic pathway was confirmed by a significant elevation in Bax/Bcl-2 ratio with 30- and 15-fold after treatment of HepG-2 cells with compounds 5 and 21 compared to the control. In addition, significant increase in the protein level concentrations of caspase-3/-7 was also observed. The most potent cytotoxic compound 5 showed promising dual inhibitory activity against VEGFR-2 enzyme with IC<sub>50</sub> value 0.59  $\mu$ M which was 4-fold more potent than Sorafenib (IC<sub>50</sub> = 2.07  $\mu$ M), and against  $\beta$ -tubulin polymerization (72% polymerization inhibition at 1.92  $\mu$ M). Molecular docking of compounds 5 and 21 at the binding site of VEGFR-2 and colchicine tubulin binding site was done to explain the exhibited inhibitory activity against both targets. Finally, quantitative structure-activity relationship (QSAR) studies delivered equation of five 3D descriptors with a good correlation between experimental and predicted IC<sub>50</sub> values ( $R^2 = 0.822$ ). This QSAR model provides as an effective technique for understanding the observed pharmacological properties. The compounds reported in this work represent potential cytotoxic agents that could help to develop more effective anticancer agents against gastrointestinal tumours.

## Acknowledgement

The authors are filled with respect to the memory of Dr. Ibrahim Abouelish, founder of Sekem Corporation. The authors are grateful to all members of the department of Cancer Biology, National Cancer Institute, Cairo, Egypt, for carrying out the cytotoxicity testing. The authors thank Dr. Esam Rashwan, Head of the confirmatory diagnostic unit VACSERA, Egypt, for carrying out VEGFR-2 inhibition assays.

## Disclosure statement

No potential conflict of interest was reported by the authors.

## ORCID

Ahmed T. Negmeldin  <http://orcid.org/0000-0003-3399-3435>

## References

1. Lanza G, Messerini L, Gafa R, et al. Colorectal tumors: the histology report. *Dig Liver Dis* 2011;43:S344–S55.
2. Gao JJ, Shi ZY, Xia J, et al. Sorafenib-based combined molecule targeting in treatment of hepatocellular carcinoma. *WJG* 2015;21:12059–70.
3. Zhang X, Raghavan S, Ihnat M, et al. The design and discovery of water soluble 4-substituted-2,6-dimethylfuro[2,3-d]pyrimidines as multitargeted receptor tyrosine kinase inhibitors and microtubule targeting antitumor agents. *Bioorg Med Chem* 2014;22:3753–72.
4. Von Felden J, Schulze K, Gil-Ibanez I, et al. First- and second-line targeted systemic therapy in hepatocellular carcinoma—an update on patient selection and response evaluation. *Diagnostics* 2016;6:44.



5. Arnold M, Sierra MS, Laversanne M, et al. Global patterns and trends in colorectal cancer incidence and mortality. *Gut* 2016;0:1–9.
6. Frenette C, Gish R. Targeted systemic therapies for hepatocellular carcinoma: clinical perspectives, challenges and implications. *WJG* 2012; 18:498–506.
7. Zwick E, Bange J, Ullrich A. Receptor tyrosine kinase signaling as a target for cancer intervention strategies. *Endocr-Relat Cancer* 2001;8:161–73.
8. Wu J, Ji J, Weng B, et al. Discovery of novel non-ATP competitive FGFR1 inhibitors and evaluation of their anti-tumor activity in non-small cell lung cancer *in vitro* and *in vivo*. *Oncotarget* 2014;5:4543–53.
9. Garuti L, Roberti M, Bottegoni G. Non-ATP competitive protein kinase inhibitors. *Curr Med Chem* 2010;17:2804–21.
10. Chen X, Lu T, Lu S, et al. Structure-based and shape-complemented pharmacophore modeling for the discovery of novel checkpoint kinase1 inhibitors. *J Mol Model* 2010;16:1195–204.
11. Farsangi MH. Small-molecule inhibitors of the receptor tyrosine kinases: promising tools for targeted cancer therapies. *Int. J. Mol. Sci* 2014;15:13768–801.
12. Chen Y, Fu L. Mechanisms of acquired resistance to tyrosine kinase inhibitors. *Acta Pharmaceutica Sinica B* 2011;1:197–207.
13. Liu Y, Gray NS. Rational design of inhibitors that bind to inactive kinase conformations. *Nat. Chem. Biol* 2006; 2:358–64.
14. Avendaño C, Menéndez JC. Drugs that inhibit signalling pathways for tumor cell growth and proliferation. *Med Chem Anticancer Drugs* 2008;251–305.
15. Blumenschein GR, Reckamp K, Stephenson GJ, et al. Phase Ib Study of motesanib, an oral angiogenesis inhibitor, in combination with carboplatin/paclitaxel and/or panitumumab for the treatment of advanced non-small cell lung cancer. *Clin Cancer Res* 2010;16:279–90.
16. Garton AJ, Crew APA, Franklin M, et al. OSI-930: a novel selective inhibitor of kit and kinase insert domain receptor tyrosine kinases with antitumor activity in mouse xenograft models. *Cancer Res* 2006;66:1015–24.
17. Yap TA, Arkenau HT, Camidge DR, et al. First-in-human phase I trial of two schedules of OSI-930, a novel multitargeted tyrosine kinase inhibitor, incorporating translational proof-of-mechanism studies. *Clin Cancer Res* 2013;19:909–19.
18. Riesterer O, Matsumoto F, Wang L, et al. A novel Chk inhibitor, XL-844, increases human cancer cell radiosensitivity through promotion of mitotic catastrophe. *Invest New Drugs* 2011;29:514–22.
19. Lowinger TB, Riedl B, Dumas J, et al. Design and discovery of small molecules targeting Raf-1 kinase. *Curr Pharm Des* 2002;8:2269–78.
20. El-Aarag BYA, Kasai T, Zahran MAH, et al. *In vitro* anti-proliferative and anti-angiogenic activities of thalidomide dithiocarbamate analogs. *Int Immunopharmacol* 2014;21:283–92.
21. Barnes TA, O’Kane GM, Vincent MD, et al. Third-generation tyrosine kinase inhibitors targeting epidermal growth factor receptor mutations in non-small cell lung cancer. *Front Oncol* 2017;7:113.
22. Hoelder S, Clarke PA, Workman P. Discovery of small molecule cancer drugs: successes, challenges and opportunities. *Mol Oncol* 2012;6:155–76.
23. Lu M, Kong X, Wang H, et al. A novel microRNAs expression signature for hepatocellular carcinoma diagnosis and prognosis. *Oncotarget* 2017;8:8775–84.
24. Nerini IF, Cesca M, Bizzaro F, et al. Combination therapy in cancer: effects of angiogenesis inhibitors on drug pharmacokinetics and pharmacodynamics. *Chin J Cancer* 2016;35:61.
25. Bates D, Eastman A. Microtubule destabilising agents: far more than just antimitotic anticancer drugs. *Br J Clin Pharmacol* 2017;83:255–68.
26. Lu Y, Chen J, Xiao M, et al. An overview of tubulin inhibitors that interact with the colchicine binding site. *Pharm Res* 2012;29:2943–71.
27. Mikstacka R, Stefański T, Róžański J. Tubulin-interactive stilbene derivatives as anticancer agents. *Cell Mol Biol Lett* 2013;18:368–97.
28. Mauer AM, Cohen EE, Ma PC, et al. A Phase II study of ABT-751 in patients with advanced non-small cell lung cancer. *J Thorac Oncol* 2008;3:631–6.
29. Hu MJ, Zhang B, Yang HK, et al. Design, synthesis and molecular docking studies of novel indole-pyrimidine hybrids as tubulin polymerization inhibitors. *Chem Biol Drug Des* 2015;86:1491–500.
30. Staben LR, Yu S, Chen J, et al. Stabilizing a tubulysin antibody–drug conjugate to enable activity against multidrug-resistant tumors. *ACS MedChem Lett* 2017;8:1037–41.
31. Nguyen TL, McGrath C, Hermone AR, et al. A common pharmacophore for a diverse set of colchicine site inhibitors using a structure-based approach. *J Med Chem* 2005;48:6107–16.
32. Zefirova ON, Diikov AG, Zyk NV, et al. Ligands of the colchicine site of tubulin: a common pharmacophore and new structural classes. *Russ Chem Bull Int Ed* 2007;56:680–8.
33. Botta M, Forli S, Magnani M, et al. Molecular modeling approaches to study the binding mode on tubulin of microtubule destabilizing and stabilizing agents. *Top Curr Chem* 2009;286:279–328.
34. Fortin S, Bérubé G. Advances in the development of hybrid anticancer drugs. *Expert Opin Drug Discov* 2013;8:1029–47.
35. Albert JS, Blomberg N, Breeze AL, et al. An integrated approach to fragment-based lead generation: philosophy, strategy and case studies from AstraZeneca’s drug discovery programmes. *Curr Top Med Chem* 2007;7:1600–29.
36. Chekler ELP, Kiselyov AS, Ouyang X, et al. Discovery of dual VEGFR-2 and tubulin inhibitors with *in vivo* efficacy. *ACS Med Chem Lett* 2010;1:488–92.
37. Wilson C, Ye X, Pham T, et al. AXL inhibition sensitizes mesenchymal cancer cells to anti-mitotic drugs. *Cancer Res* 2014;74:5878–90.
38. Elshaier YAMM, Shaaban MA, Abd El Hamid MK, et al. Design and synthesis of pyrazolo[3,4-d]pyrimidines: Nitric oxide releasing compounds targeting hepatocellular carcinoma. *Bioorg Med Chem* 2017;25:2956–70.
39. Abdelhaleem EF, Abdelhameid MK, Kassab AE, et al. Design and synthesis of thienopyrimidine urea derivatives with potential cytotoxic and pro-apoptotic activity against breast cancer cell line MCF-7. *Eur J Med Chem* 2018;143:1807–25.
40. Hu Y, Yang S, Shilliday FB, et al. Novel metabolic bioactivation mechanism for a series of anti-inflammatory agents (2,5-diaminothiophene derivatives) mediated by cytochrome P450 enzymes. *Drug Metab Dispos* 2010;38:1522–31.
41. Medower C, Wen L, Johnson WW. Cytochrome P450 oxidation of the thiophene-containing anticancer drug 3-[(quinolin-4-ylmethyl)-amino]-thiophene-2-carboxylic acid (4-trifluoromethoxy-phenyl)-amide to an electrophilic intermediate. *Chem Res Toxicol* 2008;21:1570–77.

42. Fadda AA, Bondock S, Rabie R, et al. Cyanoacetamide derivatives as sythons in heterocyclic synthesis. *Turk J Chem* 2008;32:259–86.
43. Skehan P, Storeng R, Scudiero D, et al. New colorimetric cytotoxicity assay for anticancer-drug screening. *J Natl Cancer Inst* 1990;82:1107–22.
44. El-Meligie S, Taher AT, Kamal AM, et al. Design, synthesis and cytotoxic activity of certain novel chalcone analogous compounds. *Eur J Med Chem* 2017;126:52–60.
45. Irfan M, Aneja B, Yadava U, et al. Synthesis, QSAR and anticandidal evaluation of 1,2,3-triazoles derived from naturally bioactive scaffolds. *Eur J Med Chem* 2015;93:246–54.
46. Ravichandran S, Karthikeyan E. Microwave synthesis-a potential tool for green chemistry. *Int J Chemtech Res* 2011;3:466–70.
47. Stefanidis G and Stankiewicz AJ. Energy sources for green chemistry *Alternative Energy Sources for Green Chemistry*, 1st ed. London: The Royal Society of Chemistry; 2016:1–3.
48. Gewald K, Hain U, Schmidt M. Substituierte 3,4-diamino-thieno[2,3-b]pyrrole. *J Prakt Chem* 1986;328:459–64.
49. Raslan MA, Sayed SM. Studies with Heterocyclic -Enaminoniriles: a simple route for the synthesis of polyfunctionally substituted thiophene, Imidazo[1,2-b]pyrimido[5,4-b]thiophene and Thieno[3,2-d]pyrimidine. *J Chin Chem Soc* 2003;50:909.
50. Santilli AA, Kim DH, Wanser SV. Synthesis of pyrimido[4,5-e][1,4]oxazepin-5-ones. *J Heterocyclic Chem* 1972;9: 309–453.
51. Ho YW, Yao WH. Synthesis and characterization of new pyrimidine based 1,3,4-oxa(thia)diazoles, 1,2,4-triazoles and 4-thiazolidinones. *Dyes and Pigments* 2009;2009:281.
52. Mabkhoot YN. Synthesis and chemical characterisation of new bis-thieno [2,3-b]thiophene derivatives. *Molecules* 2010;15:3329–27.
53. Tolba MF, Esmat A, Al-Abd AM, et al. Caffeic acid phenethyl ester synergistically enhances docetaxel and paclitaxel cytotoxicity in prostate cancer cells. *Int Union Biochem Mol Biol* 65 2013;65:716–29.
54. Hassan M, Watari H, AbuAlmaaty A, et al. Apoptosis and molecular targeting therapy in cancer. *Biomed Res Int* 2014;2014:150845.
55. Brentnall M, Rodriguez-Menocal L, De Guevara RL, et al. Caspase-9, caspase-3 and caspase-7 have distinct roles during intrinsic apoptosis. *BMC Cell Biol* 2013;14:32.
56. Roy K, Kar S, Narayan Das R. Understanding the Basics of QSAR for Applications in Pharmaceutical Sciences and Risk Assessment. 1st ed. 2015;70–4.